Depositional Analysis of the Uppper Meguma (Halifax Formation) at Ovens Park, Lunenburg County, Nova Scotia

by

Albert M. D'Orsay

Submitted in partial fulfillment of the requirements for the degree of Bachelor of Science (Honours)

at

Dalhousie University
Halifax, Nova Scotia

1981

DEPARTMENT OF GEOLOGY
DALHOUSIE UNIVERSITY
HALIFAX, NOVA SCOTIA
CANADA
B3H 4J1

DALHOUSIE UNIVERSITY, DEPARTMENT OF GEOLOGY

B.Sc. HONOURS THESIS

Author: Albert M. D'ORSAY

Title: DEPOSITIONAL ANALYSIS OF THE UPPER MEGUMA (HALIFAX FORMATION) AT OVENS PARK, LUNENBURG COUNTY, NOVA SCOTIA

Signature of author

Date: May 16, 1983

Distribution License

DalSpace requires agreement to this non-exclusive distribution license before your item can appear on DalSpace.

NON-EXCLUSIVE DISTRIBUTION LICENSE

You (the author(s) or copyright owner) grant to Dalhousie University the non-exclusive right to reproduce and distribute your submission worldwide in any medium.

You agree that Dalhousie University may, without changing the content, reformat the submission for the purpose of preservation.

You also agree that Dalhousie University may keep more than one copy of this submission for purposes of security, back-up and preservation.

You agree that the submission is your original work, and that you have the right to grant the rights contained in this license. You also agree that your submission does not, to the best of your knowledge, infringe upon anyone's copyright.

If the submission contains material for which you do not hold copyright, you agree that you have obtained the unrestricted permission of the copyright owner to grant Dalhousie University the rights required by this license, and that such third-party owned material is clearly identified and acknowledged within the text or content of the submission.

If the submission is based upon work that has been sponsored or supported by an agency or organization other than Dalhousie University, you assert that you have fulfilled any right of review or other obligations required by such contract or agreement.

Dalhousie University will clearly identify your name(s) as the author(s) or owner(s) of the submission, and will not make any alteration to the content of the files that you have submitted.

If you have questions regarding this license please contact the repository manager at dalspace@dal.ca.

Grant the distribution license by signing and dating below.

_____ _____

Name of signatory Date

Table of Contents

Table of contents continued...

Figures: Page

Plates:

Abstract

Two sections of the Halifax Formation, Meguma Group (Lower Paleozoic) at Ovens Park, Nova Scotia, were examined for sedimentary structures, grain size and facies associations.

Interpretation of the depositional processes and the sedimentary environment was attempted in view of modelsof sediment gravity flow and deep-sea fan deposition.

The depositional environment is in the mid-fan area of a deep-sea fan and the beds were viewed as products of turbidity flows. The recognition of Bouma (1962) Ta, Tb, and Tc equivalents (Facies A, B, and C respectively) and the presence of fine grain sediment (very fine sandstone to mudstone) suggests that the processes responsible for producing sequences with Bouma (1962) division characteristics are not restricted to sand-size sediments. The presence of beds with undulose, wavy bedding planes and beds with plane bedding suggests that there may be a distribution of "power" within turbidity flows. The wavy, undulose bedding results from the rate of deposition decreasing less rapidly with time than the rate of bed load transport. The term "low power flow" is used to distinguish strata deposited under waning flow conditions, low velocities and low sediment concentrations; the term "high power flow", is used to distinguish strata deposited under higher velocities and higher

sediment concentration than strata deposited under low power flow conditions.

Facies descriptions were related to descriptions of recent deposits of deep sea fans. Facies associations, as defined by sequence analysis, and variations in facies associations are believed to reflect changes in the power of the turbidity flow; the change in the power of the turbidity flow, the grain size and sedimentary structures recognized in each facies reflect the depositional environment of the turbidite unit.

Acknowledgements

The work of this thesis was carried out under the supervision of Dr. D. J. W. Piper, whose advice was greatly appreciated.

SECTION I - INTRODUCTION

Geology of the Meguma Group

The Meguma Group of Nova Scotia is composed of the flysch-like Goldenville and Halifax Formations (Stevenson, 1959; Campbell and Schenk, 1967). The dominant lithology of the Goldenville Formation is metasandstone with minor interbedded slates; the Halifax Formation is predominantly shale interbedded with thin sandstone layers (Stevenson, 1959).

The thickness of the Goldenville Formation (Woodman 1904) exceeds 5600 metres (Fairbault, 1914; Dwyer, 1979); the base of this Formation is not exposed. It is conformably overlain by the Halifax Formation (Ami, 1900) which is as much as 4400 metres thick (Phinney, 1961). The conformable transition of the Goldenville Formation to Halifax Formation occurs as a gradual decrease in the proportion of sandstone to shale, (Dwyer, 1979).

Paucity of fossils makes stratigraphic correlation and age determination within the Meguma Group difficult. The graptolite Dictyonema flabelliforme (Eichwald) is found in the upper section of the Halifax Formation, (Crosby, 1962) indicating an early Ordovician age for the uppermost section of the Meguma Group. Trace fossils, such as feeding trails and sand volcanoes attributed to burrowing, occur in the Goldenville Formation (Dwyer, 1979).

The major structural features of the Meguma Group are large, open low plunging synclines and anticlines trending northeast-southwest (Fyson, 1966).

Large granitic plutons have intruded the Meguma Group, metamorphosing the sediments to hornfels and andalusite schists within the pluton aureoles. Regional metamorphism has changed the shales, siltstones and quartzwackes of the Halifax Formation to slates and quartzwackes of greenschist to amphibolite schist facies (Fyson, 1966; Keppie and Muecke, 1979).

Purpose of the Study

The present study investigates a small area of the Halifax Formation and is an attempt to contribute to the questions:

1. Whether the Halifax Formation is an abyssal plain, deep sea fan, continental slope, or a continental shelf deposit.
2. Whether the Halifax Formation is a contourite or a turbidite deposit.
3. Is the Goldenville to Halifax Formation transition synchronous, supply or environmentally related.

Thesis Area and Local Geology

The thesis area is located at Ovens Park, Lunenburg County, Nova Scotia. At the Ovens Park sections of

the Halifax Formation are exposed as seacliff , polished beach and surf zone outcrop. Two sections of strata, one at Thunder Cave (Section One, Appendix One) and one at Ovens Park Beach (Section Two, Appendix Two) were chosen as the study sections. (Refer to Figure 1 for the general locations of the sections).

The strata at Ovens Park strike southwest-northeast (050-075 degrees true north) and dip from near vertical in the southern portion of the study area to 40 degrees northwest in the northern part. The examined sections are located on opposing flanks of a large anticline (Figure 1).

Two phases of deformation are recognized in the strata at Ovens Park. The dominant structure is a northeast plunging F_1 deformation consisting of an open and rounded anticline. Kink planes within the large F_1 fold indicate an F_2 generation of deformation. The F_2 generation kink planes dip southwest and develop at right angles to the bedding surface.

Small sinistral faults follow the kink planes. This suggests that faulting and kinking may be genetically related.

Regional metamorphism in the Ovens Park area is low grade; grain size and sedimentary structures are preserved in the very fine sandstone-medium siltstone units; the fine siltstone-mudstone units have been hardened by the metamorphism making sedimentary structures difficult to observe.

The examined sections represent a stratigraphic thickness of 50 metres. The lateral exposure of the bedding is limited by the horizontal exposure of the outcrop, which ranges from one to ten metres.

Previous Work

Several authors have suggested environments for the deposition of the Meguma.

Woodman suggested that a moderate, shallow, turbulent sea was the depositional environment (1904). Malcom (1929) explained the presence of interbedded sands and shales by suggesting that variations in runoff, changing current patterns and variations in the subsidence rate changed the sediment supply. Douglas et al (1938) compared graded layers in the Halifax Formation to yearly varves. The graded layers - yearly varves analogy indicated seasonal variations in the sediment supply. This was the first examination of part of the Meguma for evidence of periodic tendencies in sedimentation. Crosby (1962) also suggested seasonal variations in the sediment supply.

Phinney (1961) concluded, after examining a part of the Goldenville Formation, that the sand and shale beds were turbidites. Taylor (1967) attributed deposition of the Goldenville Formation to northwest trending turbidity currents in deep water which ceased as water depth decreased, depositing the sediment of the Halifax Formation. Campbell (1966) found a similar distribution pattern for paleocurrent

indicators. A study by Schenk (1970) indicates turbidity current distribution from a source to the southeast in a sharp right curving direction to the northeast. He suggested that deposition may have been modified by bottom currents.

Harris and Schenk (1975) suggested that there was some form of association of the Halifax and Goldenville Formations. The formations represented "distal" and "proximal" facies respectively in a deep sea fan environment. Harris and Schenk (1968) described the Goldenville Formation as fluxoturbidites that are typically thick, poorly graded sand beds showing features of rapid fluidized emplacement and down slope slumping (Harris, 1971) in some cases. They described cylic trends in sedimentation as "megarhythms" which existed vertically on a smaller scale (25m) and a larger scale (200 to 700m) (Harris and Schenk, 1975). A similar study of a section of the Goldenville was performed by Dwyer (1979) to determine the sedimentary process responsible for deposition of part of the Goldenville Formation.

Methods

The methods used in this thesis were designed to help in the study of a stratigraphic section. Grain size, sedimentary structures and bedding plane characteristics were noted. The systematic approach used in this study was:

1. Examine the outcrop section in detail and note bedding plane characteristics, sedimentary structures and paleocurrent indicators.

2. Take representative outcrop samples for thin sections, slabbing and polishing.

3. Describe the sedimentary structures seen in the slabbed samples.

4. Perform a petrographic point count of quartz grains to determine the relative mean grain size of each facies or subfacies. This relative mean grain size was related to the facies or sub-facies.

A petrographic point count of quartz grains greater than 6Ø size was used to determine the approximate grain size of each facies or subfacies. Quartz grains smaller than 6Ø were not counted because thin sections were made to a thickness of 30 microns, thus the smallest grain size that could be counted was 30 microns. The thin sections were made from block samples that were chosen as representative samples of the various facies or sub-facies. The grain size of the facies or subfacies was estimated in the field by comparison with the standard samples which had been point counted. Thus size estimates are only approximate but comparable throughout the section.

Sedimentary structures were reasonably discernable in the field. Detailed descriptions of sedimentary structures were developed from block samples that were slabbed, polished and examined in the laboratory. These block samples were

considered to be representative samples of each facies or subfacies.

The bedding plane characteristics were described in the field; wavy bedding was distinguished from planar bedding. Paleocurrent indicators exposed on bedding planes were rotated by the "pencil, elastic band and notebook" method (Potter and Pettijohn, 1963) and recorded where recognizable.

Selected stratigraphic intervals were chosen for facies sequence analysis. Sequence analysis may relate these fine grain sediments to coarser sediments.

Facies relationships and sequences can be interpreted by tallying facies transitions and converting them into probabilities. Miall (1973) uses probability matrices to describe successions of facies and their interrelationships. Cant and Walker (1975) state that the main objection to this system of matrices is that it does not show the nature of the transitions.

From the raw data, a transition probability matrix was calculated; a second matrix was calculated assuming the same abundance of facies but the abundance was in a random sequence. The probability of transitions of facies A to any other facies depends only upon the observed relative abundance of other facies. A difference matrix is calculated (observed minus random): this matrix highlights

those transitions that have a higher or lower probability of occurring than if the sequence were random.

In the construction of a facies relationship diagram the nature of the transitions can be shown by reference to the raw data and different line weights of arrows can be used to show how much more common certain transitions are. Arbitrary rejection of transitions that have a negative and/or low probability of occurring greatly simplified the diagram.

SECTION II - SEDIMENTOLOGICAL PROCESSES

Processes of Mass Gravity Transport

In the deep sea environment much of the sediment moves by mass gravity transport under the direct influence of gravity forces.

The mechanics of sediment failure and the geological conditions that trigger failure can explain mass-gravity transport in the deep seas. When sediments are deposited on a slope surrounding a deep-sea basin they will move downslope only when shear stress exerted by the force of gravity exceeds the shear strength of sediment. Shear strength is defined as a function of the cohesion between the grains plus intergranular friction (Rupke, 1978).

Shear stress can result from several factors:

1. A steepening of the slope caused by undercutting by waves or currents or by slope failure further downslope.
2. Thickening of the sediment pile by deposition.

A decrease in shear strength can be the result of several factors:

A) An increase in pore fluid pressure leading to sediment fluidization.

B) Thixotropic behavior: a process in which the gel-sol transition takes place. Fluidization and thixotropy can be induced by strain created by shock or mechanical impact.

A substantial thickness and weight of sediment must accumulate before failure occurs on a slope; geologic

conditions that trigger failure tend to be periodic or episodic.

Mass gravity transport can be divided into three types.

1. Rock falls
2. Sliding and slumping
3. Sediment gravity flow
   a) debris flow
   b) grain flow
   c) fluidized sediment flow
   d) turbidity flow

(Refer to Fig. 2 for a schematic classification of sedimentary gravity flows)

Only fluidized sediment flow and turbidity flow will be considered, since they are the processes most applicable to deposition in the deep sea.

Fluidized Sediment Flow

Fluidized sediment flows are created when the metastable grain fabric of a fluid-sediment mix collapses. The grains no longer form a supportive framework, but are, in part, supported by the pore fluid. In fluidized sediment flow, the grains become suspended and the sediment strength is reduced to zero.

Deposition of fluidized sediments occurs by a gradual solidification from the bottom to the top of the flow with little grain segregation occurring. The common depositional features of these flows are poor grading, sharp bottom and top, no traction structures, basal load casts, dish and pillar structures

(fluid escape structures), sand volcanoes and convolute laminations (Lowe, 1975; Middleton and Hampton, 1976.)

Turbidity Flow

Turbidity flows are a form of density current in which the excess density that drives the current is due to suspended sediment. The density of the surrounding fluid is nearly the same as that of the turbulent suspension (Knapp and Bell, 1941).

A turbidity current moves downslope along the bottom because the tangential attraction of gravity in the suspended sediment is sufficient to keep the grains in turbulent suspension and to cause the mass to flow as a denser fluid in an underflow or, if it encounters a denser watermass, it may spread out along the top as an interflow (Gould, 1951). A turbidity current ceases to exist and flow when enough of the suspended load has been deposited so that the density of the mass no longer exceeds the density of the surrounding fluid.

The main difference between turbidity currents and other resedimentation mechanisms is that turbidity currents transport their sediment load in suspension (Kuenen , 1956).

Turbidity currents are classified into low density and high density types on the basis of the non-suspension and suspension of sediment (Kuenen , 1951; Rupke, 1978). Low density turbidity currents tend to be relatively slow

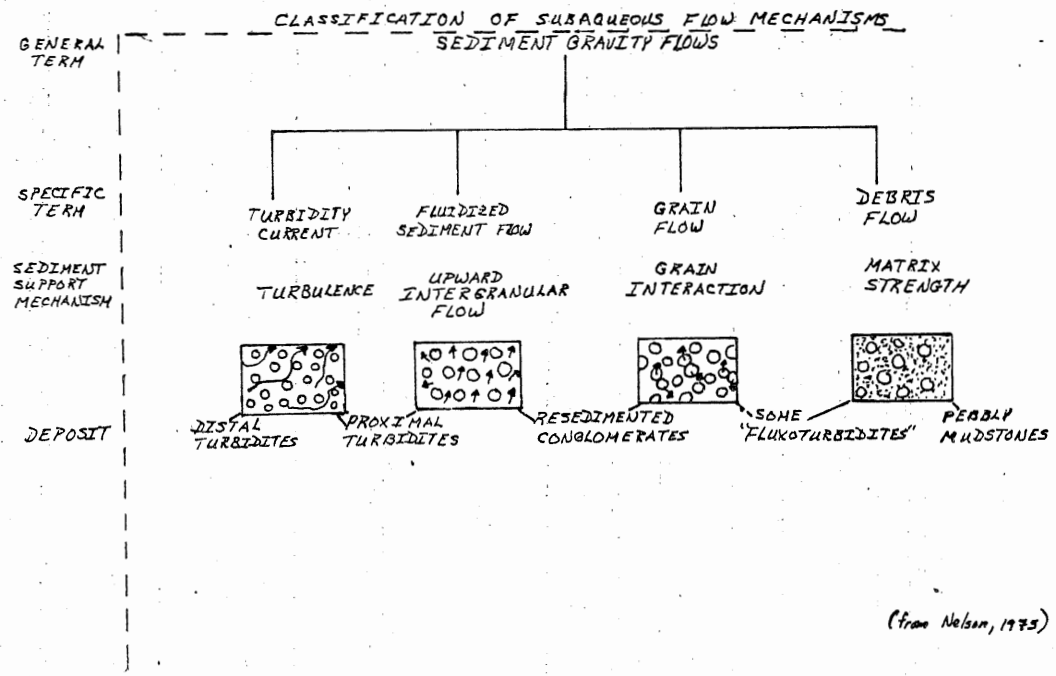

Figure 2: Schematic classification of Sediment Gravity Flows. Turbidity currents produce "distal" and "proximal" deposits. Distal turbidites have a finer grain size than proximal turbidites (from Nelson, 1975).

and long-lived. Their suspended sediment load is largely silt and clay material. High density turbidity currents tend to be relatively fast and short lived. They transport mostly sand and coarse silt particles.

Turbidite Deposits

A turbidity current denotes a density current flow down a subaqueous slope; it can spread horizontally because suspended sediment gives it a higher density than the surrounding water. A sedimentary deposit resulting from the deposition of a turbidity current is called a turbidite or turbidity deposit.

Bouma (1962) made a comprehensive study of turbidites and developed a turbidite facies model. An ideal single turbidite consists of five units with certain sedimentary structures unique to each unit. (Refer to Figure 3 for a diagrammatic presentation).

1. Graded Interval (Ta) - Lowermost part of a Bouma sequence--it shows graded bedding, although it may be indistinct in well-sorted beds. It often has a sandy texture.

2. Lower Interval of Parallel Lamination (Tb) - Exhibits thick, parallel laminae of sand size material. It usually shows a gradual contact with the lower graded interval.

3. Current Ripple Lamination Interval (Tc) - This interval consists of fine sand-coarse silt sediments showing small current ripple bedding. Climbing ripples, trough cross-stratified

ripples and convolute, laminations are usually present. The contact with the lower interval of parallel lamination is often sharp.

4. Upper Interval of Parallel Lamination (Td) - This zone of fine sand to silty clay shows a distinct parallel lamination. It has a distinct contact with the zone of current ripple lamination.

5. Pelitic interval (T_E) - This is a zone of siltstone, clayey siltstone or mudstone. It does not show any distinct sedimentary structures. Sand content and grain size decreases towards the top and it has a gradational contact with the lower interval.

Bouma (1962) remarked that a complete turbidite sequence can only be found in the thick layers of turbidite deposits. The most common occurrences are incomplete sequences where the top or bottom intervals may be missing.

Turbidite muds and silts of deep sea fans and abyssal plains are a major component of deep sea terrigenous sediment sequences (Piper, 1978). Piper (1978) divided turbidite silts and muds into four divisions. (Refer to Figure 3 foradiagrammatic presentation).

1. Laminated muds (E_1) - This division immediately overlies sand beds. The laminae are 0.2 mm to 2mm thick and consist of alternating silt and silty clay. Individual laminae are often lenticular. Some silt laminae are sharp based, others

grade up from the mud laminae with coarse flat particles concentrated at the tops of laminae (Piper, 1972).

2. Graded Mud (E_2) - This division is found either above the laminated mud or directly overlying sand. It shows an upward decrease in grain size that is often accompanied by petrographic changes. The mud usually lacks visible primary sedimentary structures or shows very indistinct bedding. Grading is often pronounced in beds with substantial amounts of very fine carbonate. Thicknesses of graded muds can be up to 20 cm. Graded muds that rest directly on earlier turbidites or non-turbidite sediment have a distinct basal zone of silty mud.

3. Ungraded Mud (E_3) - This division overlies graded mud. No systematic primary gradation in grain size or petrology is detectable. Bioturbational mixing with hemipelagic sediments masks gradational trends in hemipelagic muds.

4. Hemipelagic Sediment (F) - This division consists of pelagic sediments that settle to the bottom of the sea.

Stow and Shanmugam (1980) outlined a sequence of sedimentary structure in an idealized fine-grained turbidite unit. Nine structural divisions were identified as T_0 through to T_8. (Refer to Figure 3 for a diagrammatic presentation). Sedimentary structures were used to define the divisions.

Basal silt lamina (T_0) - Characterized by fading ripples, micro-cross and parallel lamination and sharp-scoured load cast base.

Convolute laminae (T_1) - Dominantly muddy; contains thin silt laminae which thicken immediately in front of the subjacent fading ripple crest or which are convoluted "in-phase" with the ripples.

Thin irregular laminae (T_2) - Dominantly muddy; characterized by low amplitude climbing ripples.

Thin regular laminae (T_3) - Dominantly muddy; laminae of silt are regular in thickness.

Indistinct laminae (T_4) - Dominantly muddy; laminae of silt are thin and wispy.

Wispy, convolute laminae (T_5) - Dominantly muddy; laminae of silt are thin and wispy.

Graded mud (T_6) - Dominantly muddy; fining upwards to mudstone with patchy fine silt lenses.

Ungraded mud (T_7) - Ungraded homogenous mud with rare coarse silt pseudonodules.

Micro-bioturbated mud (T_8) - Mud with microburrowing and silt pseudonodules.

The basal (lenticular) silt laminae (To) is the thickest structural unit (about 8mm) and coarsest (coarse silt-very fine sand) with a sharp irregular base. Stow and Shanmugam (1980) equated their To-T_5 divisions to E_1 of Piper (1978), T_6 to division E_2 of Piper (1978), T_7 to division E_3 of Piper (1978), and T_8 to division F of Piper (1978).

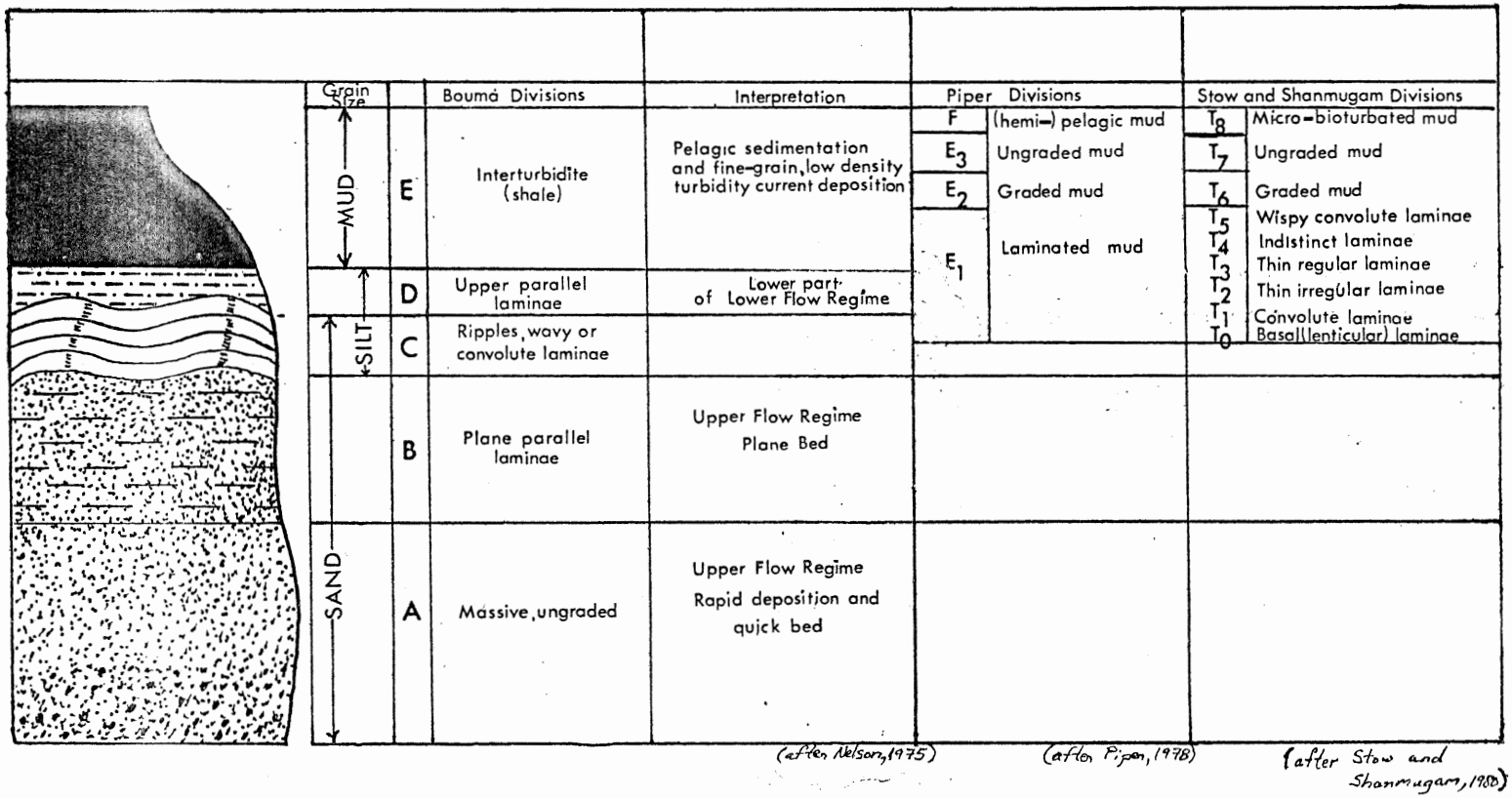

Figure 3: An illustration of the relationships between the Bouma Sequence, Piper's (1978) divisions for fine grain turbidites and the divisions of Stow and Shanmugam (1980) for fine grain turbidites. Bouma (1962) and Stow and Shanmugam (1980) base their classifications on sedimentary structures; Piper (1978) based his classification on the grain size distribution and sorting characteristics in Recent, fine grain turbidites.

The Contourite versus Turbidite Problem

Stow and Lovell (1979) noted that a lack of suitable criteria for the identification of contourites has lead to the paucity of interpretive literature on contourite deposits. Criteria developed by Piper and Brisco (1975) and Stow and Lovell (1979) were used to determine whether the measured sections were contourite or turbidite deposits. A summary of these criteria is listed below.

1. Rapidly deposited sequences (suggested by climbing ripples with no stoss side erosion) are probably of turbidite origin (Piper and Brisco, 1975).

2. Contourites are dominantly homogeneous and have poorly defined bedding (Stow and Lovell, 1979).

3. Evidence of limited sediment supply (such as "starved" ripples and scours not filled with coarse sediment (Piper and Brisco, 1975)) suggest deposition from contour currents.

4. Muddy contourites are dominantly silty muds that are medium to poorly sorted and ungraded; sandy contourites are dominantly silt to sand size; they are well sorted and relatively free of mud (Stow and Lovell, 1979).

5. Highly turbulent (erosive) flows suggest a turbidite origin (Piper and Brisco, 1975).

6. Burrows and bioturbational mottling are more common in contourite sediments than in turbidite sediments (Stow and Lovell, 1979).

The sedimentary strata at Ovens Park are dominantly mudstone with laminae of siltstone. Bedding is well defined and erosive features, such as scour channels and truncated cross-laminations, were frequently observed. Rapidly deposited sequences, which were evidenced by climbing ripples, are common. No evidence of burrowing or bioturbational mottling could be found in the measured sections and an overall fining up sequence was observed in the strata at Thunder Cave. These observations suggest that the strata at Ovens Park are turbidite in origin.

Schenk (1970) and Harris and Schenk (1975) suggest that bottom currents may have been important in the deposition of the Lower Paleozoic Meguma Group of Nova Scotia but Stow and Lovell (1979) argue that Schenk based his argument on analysis of regional sedimentation patterns within the Meguma Group, rather than on the recognition of any particular sediment facies that would be analogous to modern contourites.

SECTION III - FACIES

Facies Description

The term facies(or facies unit)is used to define a distinct section of strata that forms under certain conditions of sedimentation and reflect a particular process or environment (Reading, 1978). By using the facies concept it is possible to subdivide the facies into subfacies or group them into facies associations or assemblages.

The thicknesses of the facies units were measured to the nearest 0.5 $\pm$ 0.25cm. This was deemed as an appropriate scale for several reasons.

1. Many significant rhythmic units were found to be as thin as 0.5 $\pm$ 0.25 cm.
2. Unit thickness varies, units thinner than 0.5cm were found to be undulose and intermittent, making their lateral continuity difficult to establish.

The term grainstone is used to describe the granular (very fine sandstone to fine siltstone) sediments of the facies and subfacies. The definition of grainstone used in carbonate sedimentology is used to define the granular component of these facies; the term describes the coarse grain components that lack mud and are grain supported (Dunham, 1962).

The criteria used to define the facies assemblages were:

1. grainstone: shale ratio
2. regularity of bedding
   i) planar bedding
   ii) undulose bedding
3. sedimentary structures

4. grain size

5. homogeneity of the outcrop (i.e., is it predominantly one sediment type (sandstone, siltstone, mudstone); are there thin alternating sequences of siltstone, shale and sandstone in a unique combination such as sandstone-siltstone-shale; siltstone-shale; sandstone-shale-sandstone-shale).

Facies A - Units of facies A exhibit planar bedding and appear massive in outcrop exposures. Mudstone and siltstone clasts are frequently observed suspended within this facies unit (Plate 1a, 1b).

Petrographic thin section point count analysis of representative samples of facies A indicate that it is a very fine sandstone-coarse siltstone, (Appendix 3) with the dominant sediment component being quartz. This quartz is varied in size and shape but is generally quite angular and shows pronounced undulatory extinction. Point counting also indicates that normal and reverse grading occur in facies A.

Facies B - Units of facies B have planar bedding and exhibit a coarse, parallel laminated texture (Plate 2a, 2b).

Thin section point count analysis of representative samples of facies B indicates that it is a very fine sandstone-coarse siltstone (Appendix 3) with the dominant sediment component being similar to facies A.

The outcrop texture of facies B suggests that it is a massive, parallel laminated quartzite.

Facies C - Units of facies C have well-developed ripple

laminations (i.e., cross-laminations, trough cross-laminations, climbing ripples). Facies C is divided into two subfacies: subfacies C_1 exhibits planar bedding; subfacies C_2 exhibits wavy bedding (Plates 3a, 3b, 4a, and 4b). Wherever facies C was observed to be in contact with facies B, the contact was abrupt.

Facies C is a coarse to medium siltstone (Appendix 3) that is approximately 95% grainstone and 5% fine, micaceous clay. The dominant sediment component is quartz; secondary sediment components are detrital muscovite and feldspar. The texture of the quartz grains associated with facies C is similar to the quartz grains found in facies A.

The outcrop texture of subfacies C_2 and C_1 suggests that it is a massive, cross-bedded, quartzite that has a minor amount of mudstone in its laminae.

Facies D - Facies D consists of thin, alternating strata of grainstone and shale (Plates 5a, 5b); the monotonous grainstone units were 2.5 cm thick or less, the shale units were 5 cm thick or less. The grainstone component consists of medium to coarse siltstone (Appendix 3) the shale component is composed of dark grey, medium to fine siltstone and mudstone.

Facies D is divided into two subfacies. Subfacies D_1 has planar bedding while D_2 shows wavy bedding. Subfacies D_1 exhibits planar bedding (i.e., there is one

planar bedded mudstone or fine siltstone unit followed by a medium to coarse siltstone unit that has planar bedding); each of these units exhibits a sharp contact between each other (Plate 5a). Subfacies D_2 exhibits wavy, undulose bedding (Plate 5b). There is a fining upward coarse to medium siltstone to a fine siltstone-mudstone sediment size distribution.

Sedimentary structures, associated with facies D are climbing ripples (Figure 4) planar laminations (Figure 5) flute marks (Plate 6a), asymmetric ripple marks, ball and pillow structures (Plate 7), load clasts, convolute laminations (Plate 6b) and small scour channels (Figure 4). Fining upward sequences are characteristic of facies D.

Contacts of facies D with facies C can be either sharp or gradational; the contact of facies D with other facies is usually abrupt.

Facies E - Facies E consists of fine siltstone and mudstone with minor amounts of grainstone. It has a very low grainstone to shale ratio. Facies E is divided into three subfacies, which are denoted as subfacies E_1, subfacies E_2, and subfacies E_3.

Subfacies E_1 is a fine siltstone-mudstone unit (Appendix 3) with regular laminations of fine sandstone-medium siltstone. The laminations comprise less than twenty percent of each measured E_1 unit. The laminae are planar and measured thicknesses are from 1mm to 5mm (Plates 8a, 10).

Subfacies E_2 is texturally similar to subfacies E_1 except that the fine sandstone-medium siltstone laminae are irregular (wavy) and that lenticular, discontinuous layers of lenses of fine sandstone to medium siltstone are apparent (Plates 8b, 10).

Subfacies E_3 is a monotonous, homogeneous, planar bedded unit of dark grey to black clayey siltstone-mudstone (Plate 9). No sandstone-medium siltstone laminae are apparent in subfacies E_3.

Facies E may have gradational or abrupt contacts with facies A, B, C, or D.

The sedimentary structures associated with subfacies E_1 were in the laminations of the fine sandstone to medium siltstone. These structures consisted of horizontal and inclined laminations. Shale laminae were frequently observed in the thin grainstone layers. Subfacies E_2 had bulbous and lenticular laminae (Plate 8b) in which starved ripples and winnowed beds were observed. The lenticles. of subfacies E_2 showed fine cross-laminations. The cross laminations within the beds are very fine and difficult to photograph, but were easily observed in the field.

Plate 1a

Plate 1b

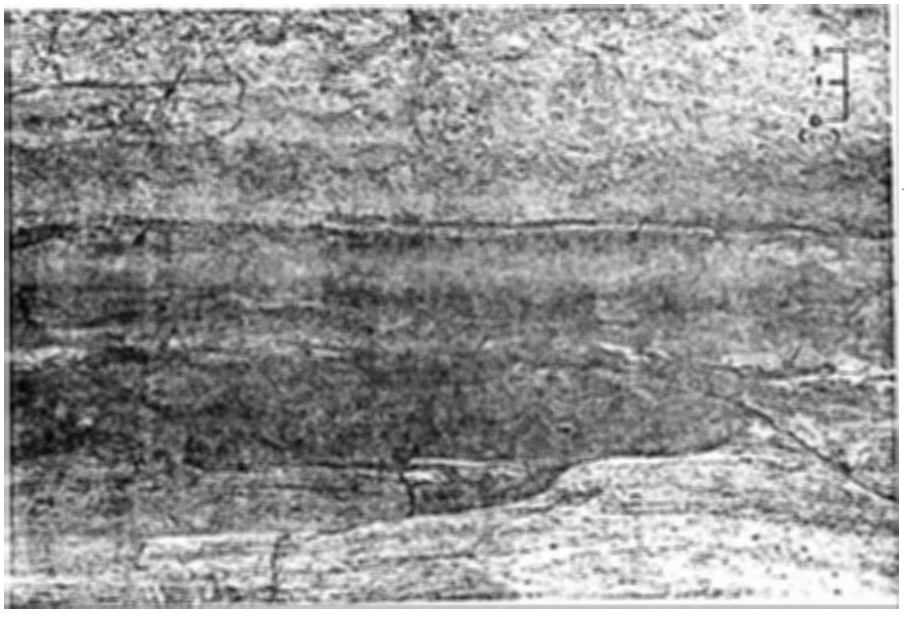

Plate 1a: shows the massive texture of facies A

Plate 1b: Arrows in plate 1b denote the mudstone intraclasts that are characteristic of facies A.

Plate 2a

Plate 2b

Plate 2a: shows the rhythmic layering of facies A and facies B.

Plate 2b: exhibits the coarse, parallel laminated texture associated with facies B.

Plate 3a

Plate 3b

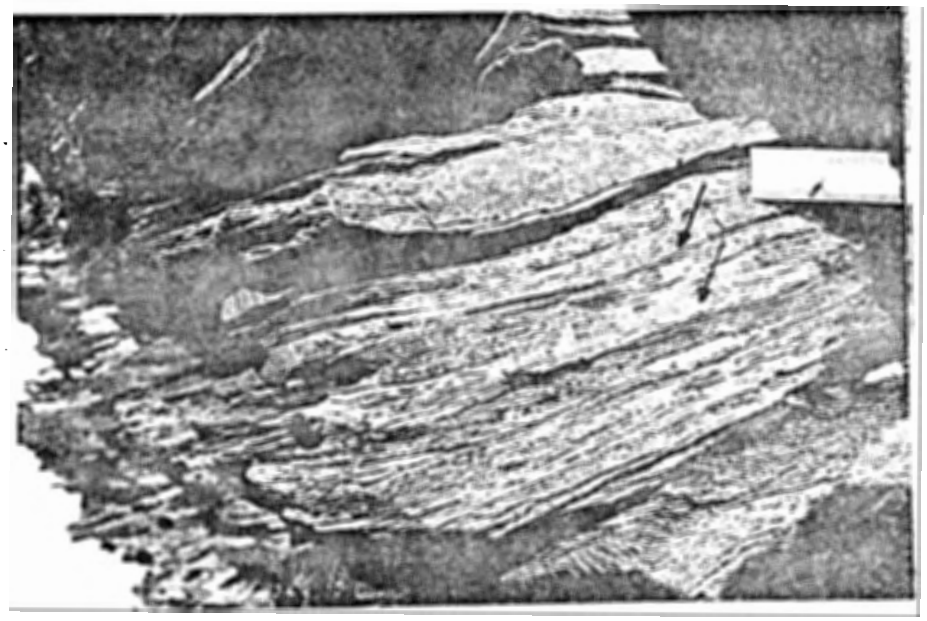

Plate 3a: shows a thick planar bedded Facies C unit (subfacies C_1). Tops is to the top of the photo and the top and base of the unit are denoted by arrows.
Plate 3b: The arrows in this photo denote two thin planar bedded units of facies C (subfacies C_1). Both photos were taken at Thunder Cave.

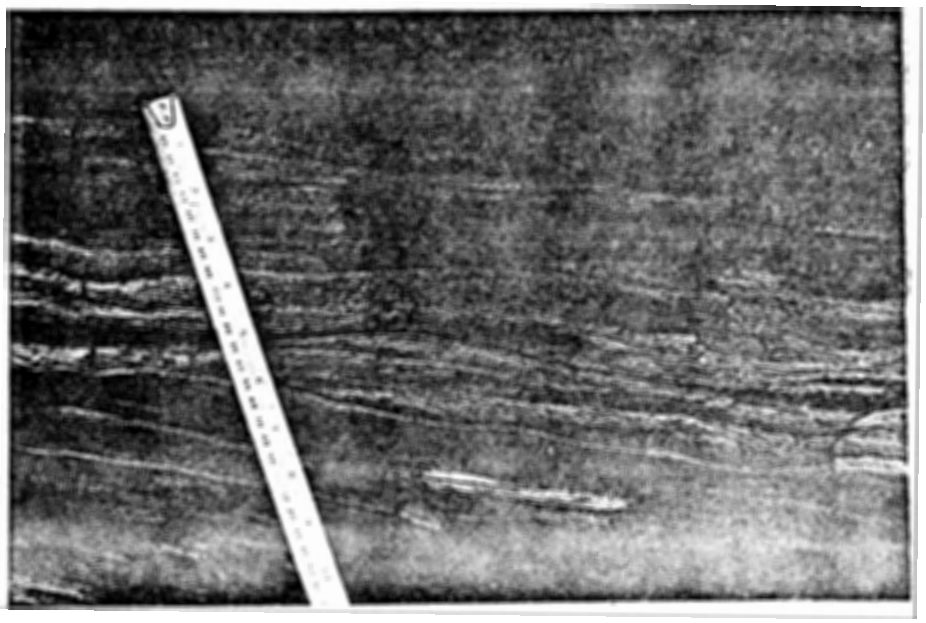

Plate 4a

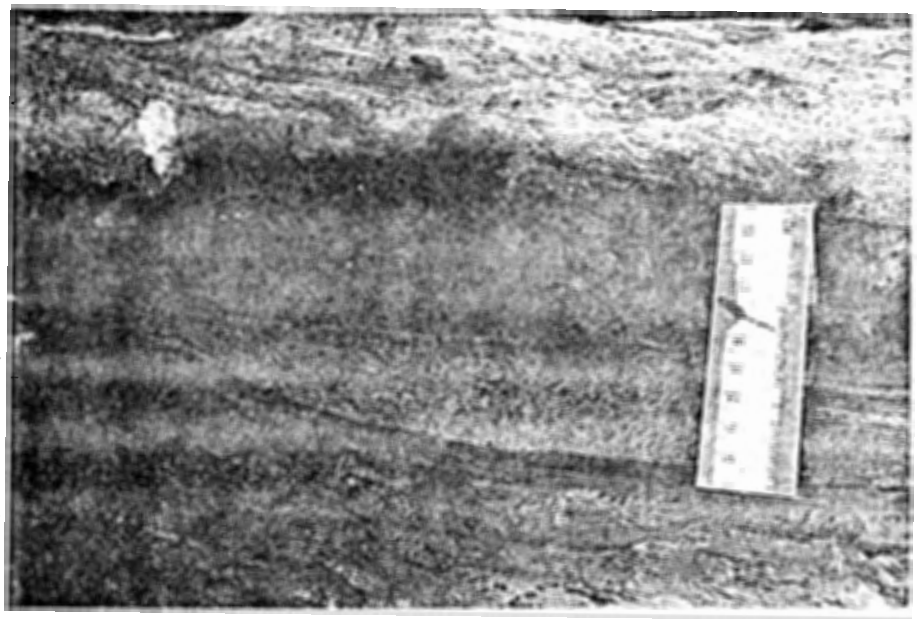

Plate 4b

Plate 4a: shows two wavy undulose beds of facies C (subfacies C_2) unit separated by a thin mudstone layer. The observed scale is approximately 1.5 cm wide.

Plate 4b: exhibits a thin mudstone layer infilling a ripple trough of a subfacies C_2 unit. The amplitude of the ripple is approximately 3.5 cm . Both photos were taken at Thunder Cave.

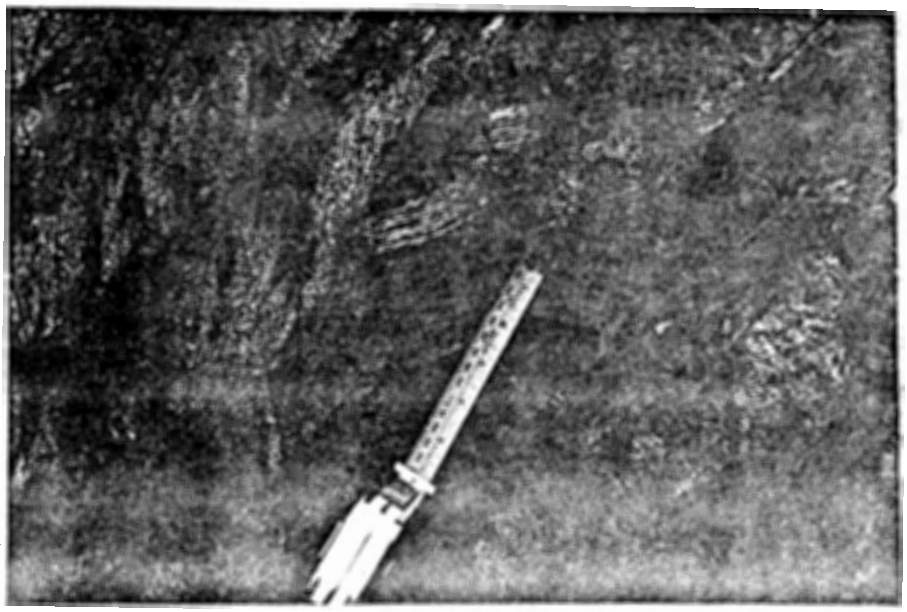

Plate 5a

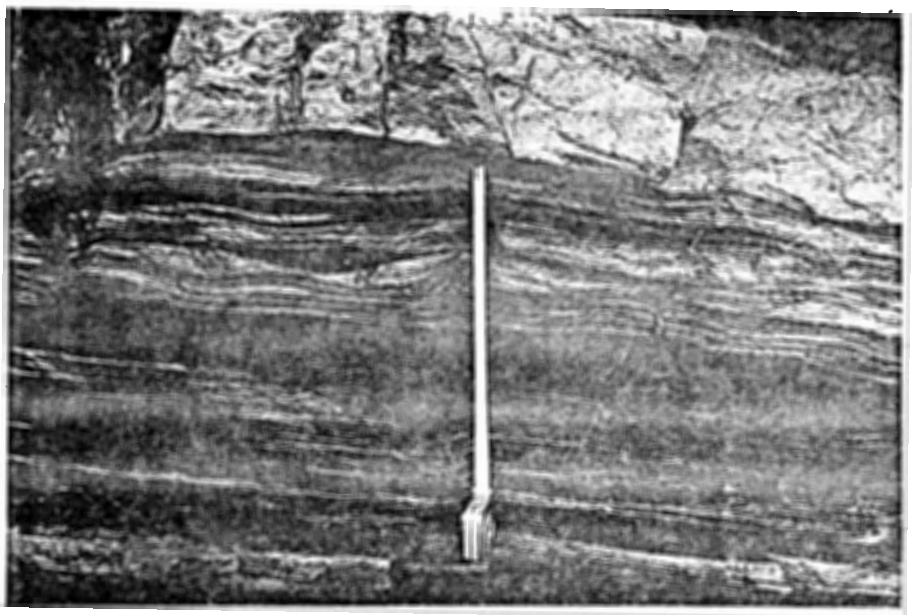

Plate 5b

Plate 5a: exhibits a subfacies D_1 unit.
Plate 5b: exhibits a subfacies D_2 unit. Note the rhythmic, alternating mudstone and grainstone units. These two photos were taken at Thunder Cave.

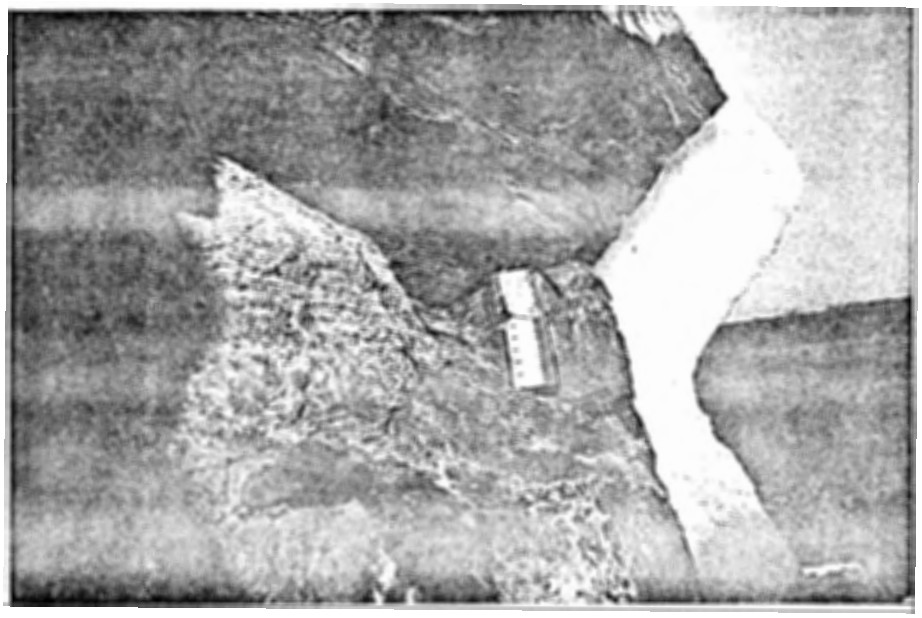

Plate 6a

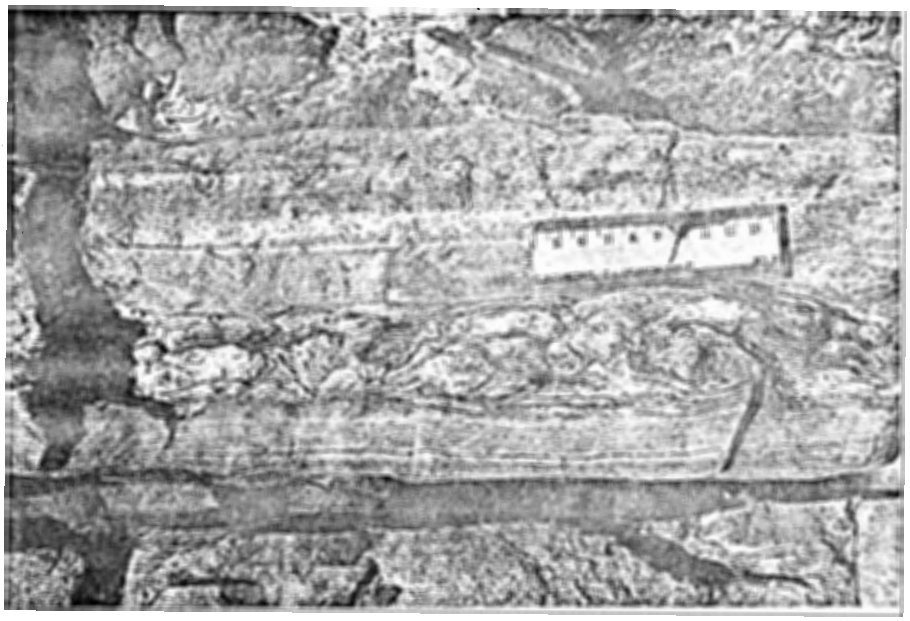

Plate 6b

Photos showing various sedimentary structures associated with facies D. In plate 6a, the arrow denotes a flute mark; convolute laminations are exhibited in plate 6b. These two photos were taken at Thunder Cave.

Plate 7

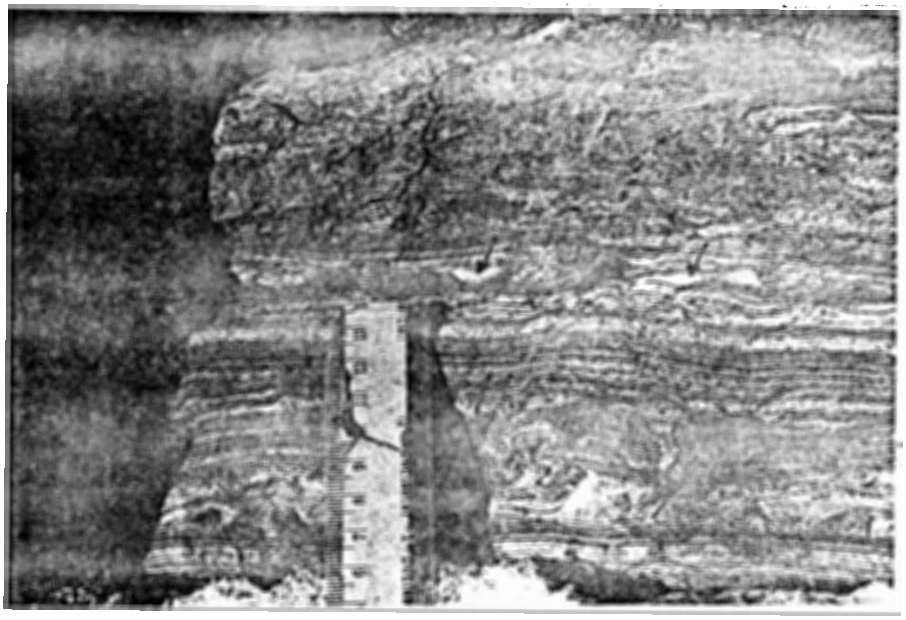

In plate 7, ball and pillow structures are denoted by the arrows. These ball and pillow structures are associated with subfacies D_1. This photo was taken at Thunder Cave.

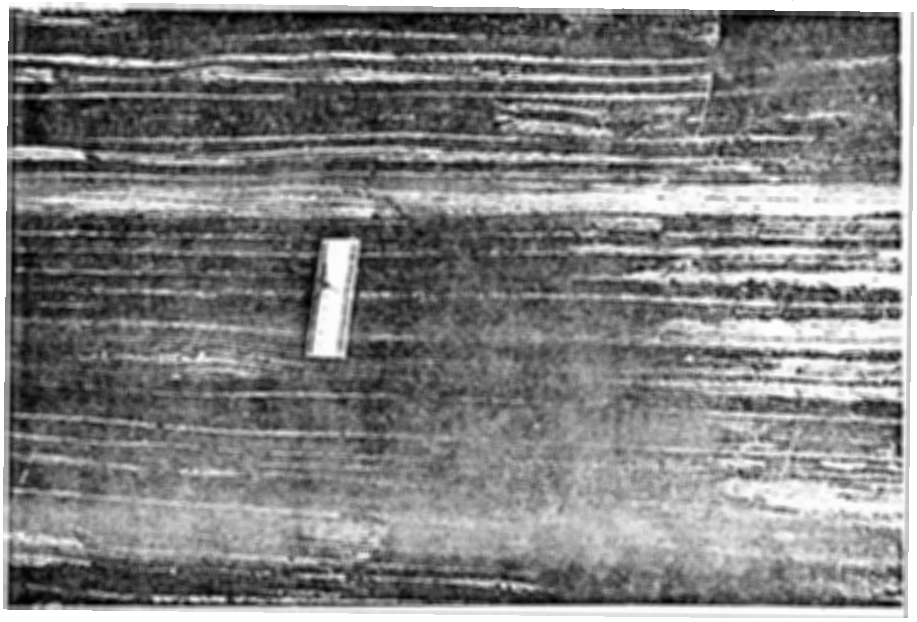

Plate 8a

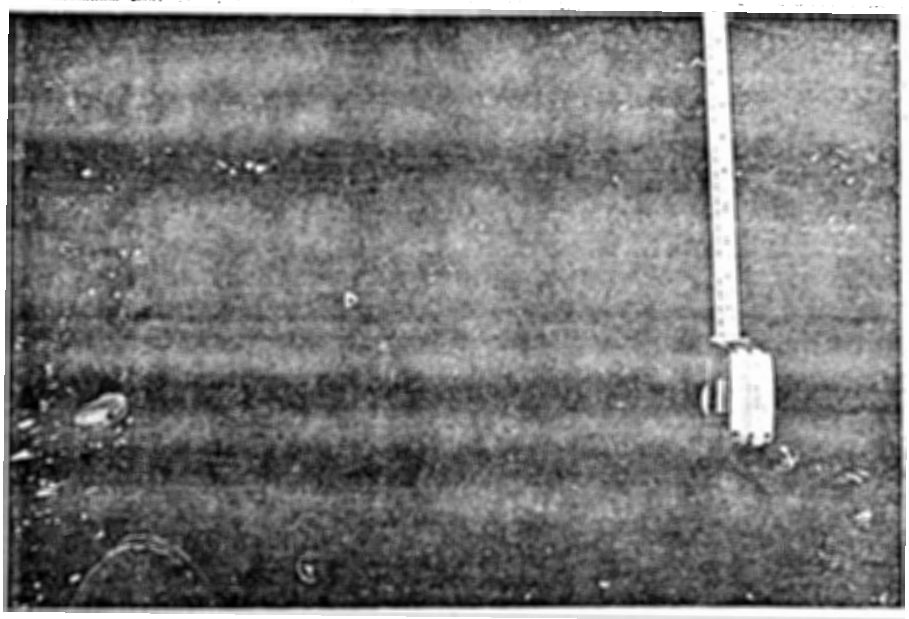

Plate 8b

Facies E is exhibited in plate 8a and plate 8b. The zone denoted by the parenthesis in plate 8a shows a typical subfacies E_1 unit. The arrows in plate 8b highlight lenticular and wavy bedding that is a characteristic of subfacies E_2. These two photos were taken at Overs Park Beach.

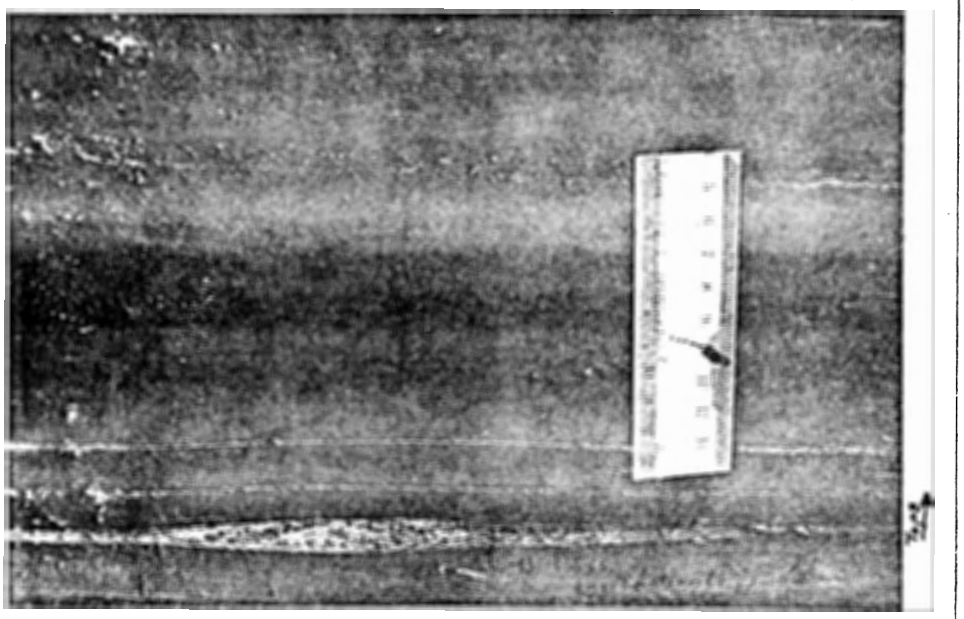

Plate 9

In plate 9, the parenthesis highlight a subfacies E_3 unit. This unit is underlain by subfacies E_1 and overlain by subfacies E_1. This photo was taken at Ovens Park Beach.

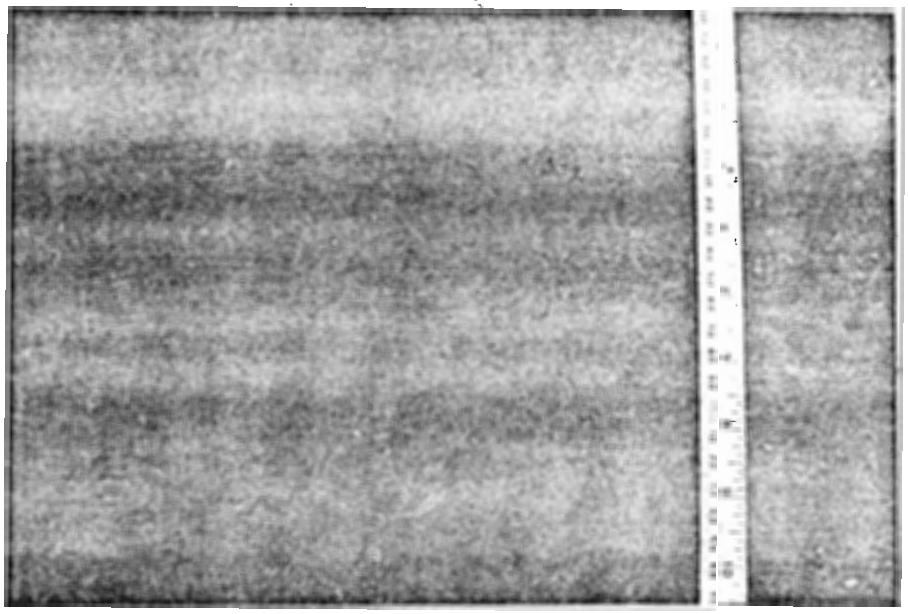

Plate 10

Plate 10: parallel laminated E_1 units are visible in the top and the middle of the photo. Other facies units that are visible are C_1, C_2, D_2, and E_2. The scale is approximately 1.5 cm wide. This photo was take at Ovens Park Beach.

Internal Structures

Internal structures are common in most beds but detailed examination of polished slabs indicates that outcrop exposures of internal structures can be deceptive, producing erroneous conclusions as to the sedimentary structures in a facies.

Cross laminations of Facies D_1, for example, are not distinguishable at the outcrop but can be readily observed in polished slab samples. At the outcrop, the coarse siltstone-medium siltstone component of facies D appears parallel laminated. Detailed examination of two representative polished block samples of facies D indicate that the parallel laminations pass up from wavy laminations. Examination of polished slab allow various sedimentary structures to be discerned that could not be seen in outcrop. The depositional environment of the facies that is being studied can be more readily interpreted by the detailed examination of the polished slabs.

(i) Graded Bedding: Graded bedding is apparent in all facies except facies C and E. The fine grain texture of the facies makes outcrop inspection for graded bedding difficult; graded bedding can only be recognized from data derived from thin section point counts. Positive and reverse graded bedding have been observed in facies A; facies B and D exhibit positive grading.

(ii) Parallel Laminations: Coarse, distinct and indistinct

laterally continuous, parallel laminations are associated with facies B. The parallel laminations vary from 0.5 to 10 mm in thickness, are more commonly diffuse than well defined and are only 0.5 to 4.0 mm apart (Plate 2b). Lighter and darker color differences define laminations which have little apparent variations in grain size. The color differences reflect increases and decreases in clay content.

(iii) Cross laminations: Cross laminations are common and occur in two types.

A. Cross laminations composed of sediment with little difference in grain size.

B. Cross laminations that alternate coarse siltstone and mudstone.

The cross laminations that are composed of sediment with little variation in grain size are in the form of prograding and climbing ripples. Cross laminations that alternate coarse siltstone and mudstone are represented by scour channels and trough cross-stratification. Climbing and prograding ripples are associated with facies C, while trough cross-laminations are found in facies C and D. Scour channels are only seen in facies D and can only be distinguished in polished rock slabs.(Figure 4).

(iv) Wavy Laminations: Wavy laminations are rare; they occur in medium to fine siltstone units and have only been observed in Facies D.(Figure 5).

(v) Convolute Laminations: Convolute (contorted) laminations

are rare, having been observed only in facies D. Convolute laminations are interpreted as deformation of semi-liquified sediment by depositional loading (Dzulynski and Walton, 1965).

(vi) Mud Clasts: Fine siltstone-mudstone lenticular inclusions are found individually or clustered in facies A. They are two to fifteen centimetres long and up to three centimetres thick. They are most commonly found near the base of a facies A unit (Plates 1a, 1b). Mud clasts are interpreted to be rip-ups from mud deposited from previous sediment flows. Middleton and Hampton (1976) associated mud clasts with fluidized flows.

(vii) Ripples: Bedding planes occasionally exhibit asymmetric ripples that have sharp crests and amplitudes of one to twenty millimetres. These ripples are most commonly observed in facies D; large amplitude ripples (0.5 - 4.0 centimeters) were observed in facies C (Plate 3b).

The ripples associated with facies D have graded mud collecting in the troughs and sand and silt size particles collecting on the stoss side; laminations are continuous but change composition from the stoss to the lee side of the ripple. These ripples are referred to by Stow and Shanmugam (1980) as fading ripples. The ripples associated with facies C were climbing ripples and prograding ripples; trough cross laminations are associated with facies C (Figure 6, 7).

Discontinuous fine sandstone to coarse siltstone lenticles were observed in subfacies E_2. These discontinuous

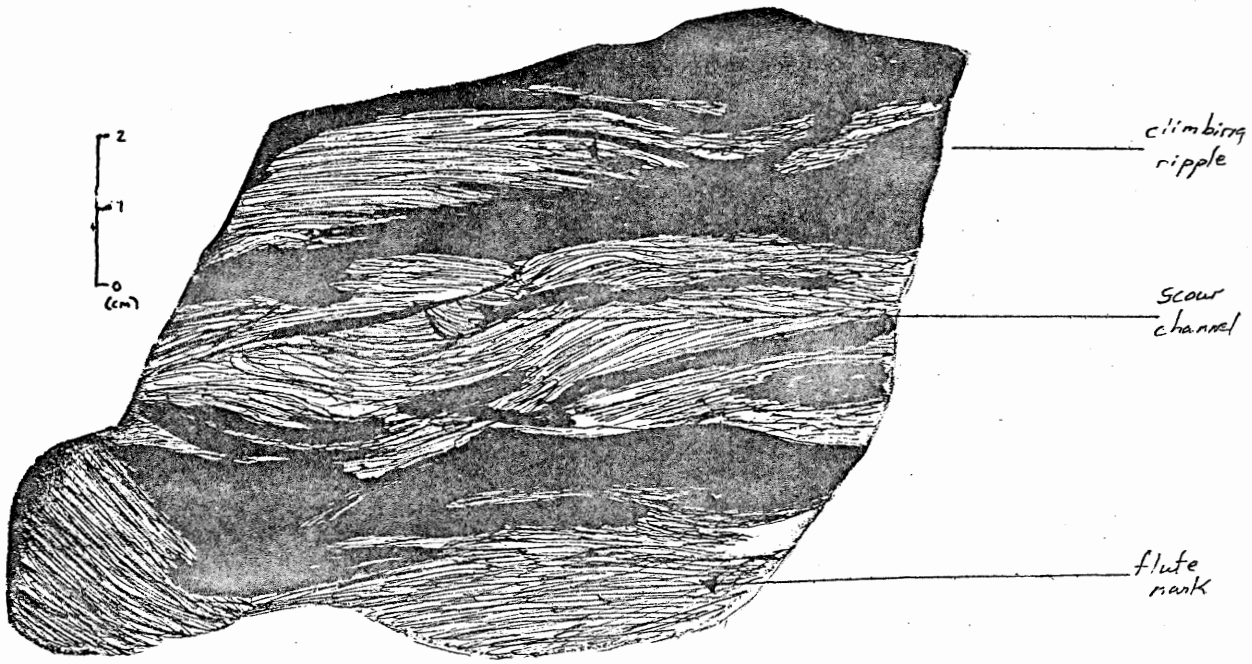

Figure 4: Sketch of a polished slab, Facies D. Sedimentary structures are noted around the diagram. Black regions represent areas of mudstone accumulation.

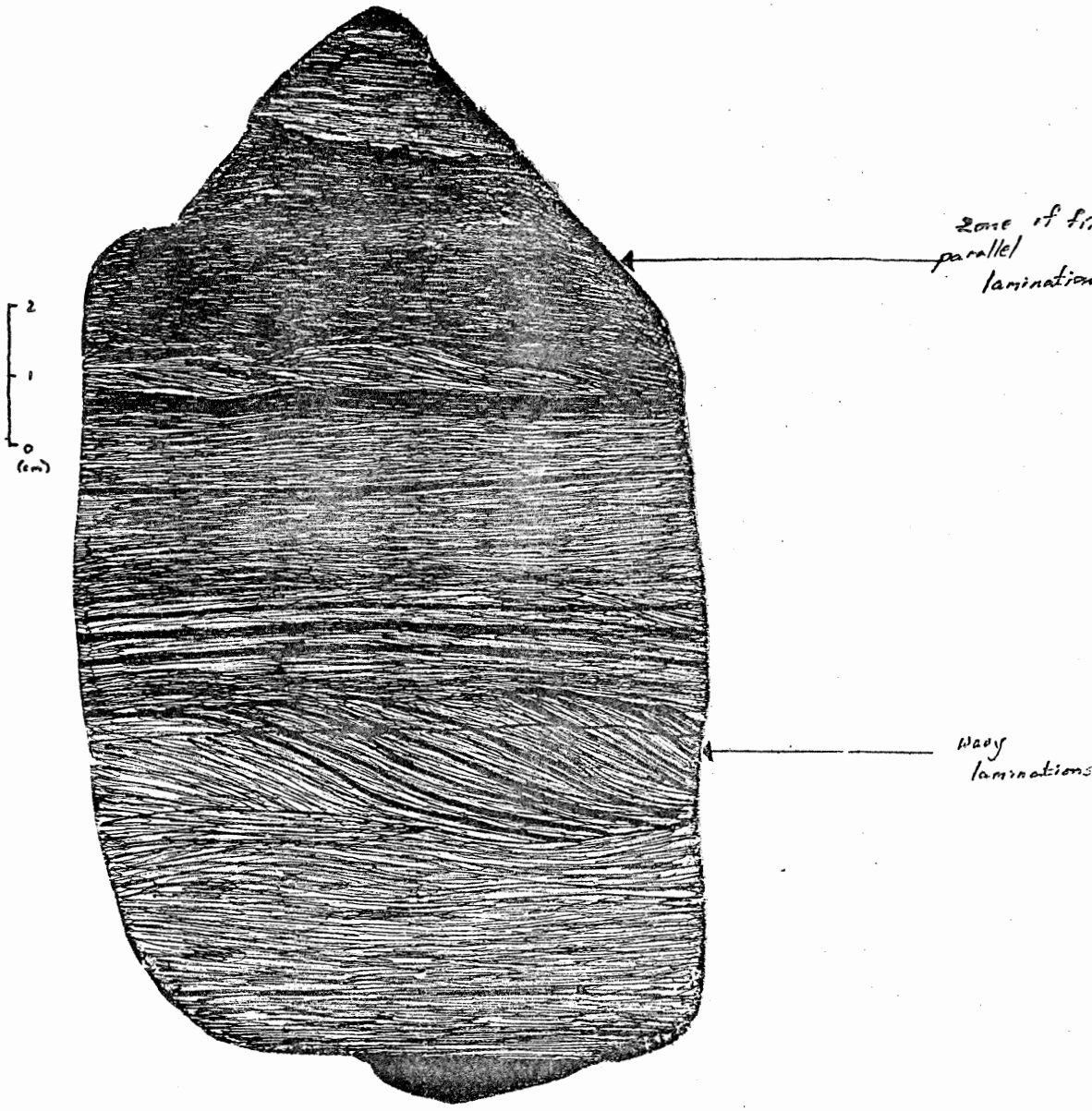

Figure 5: Sketch of a polished slab, Facies D. Sedimentary structures are noted around the diagram.

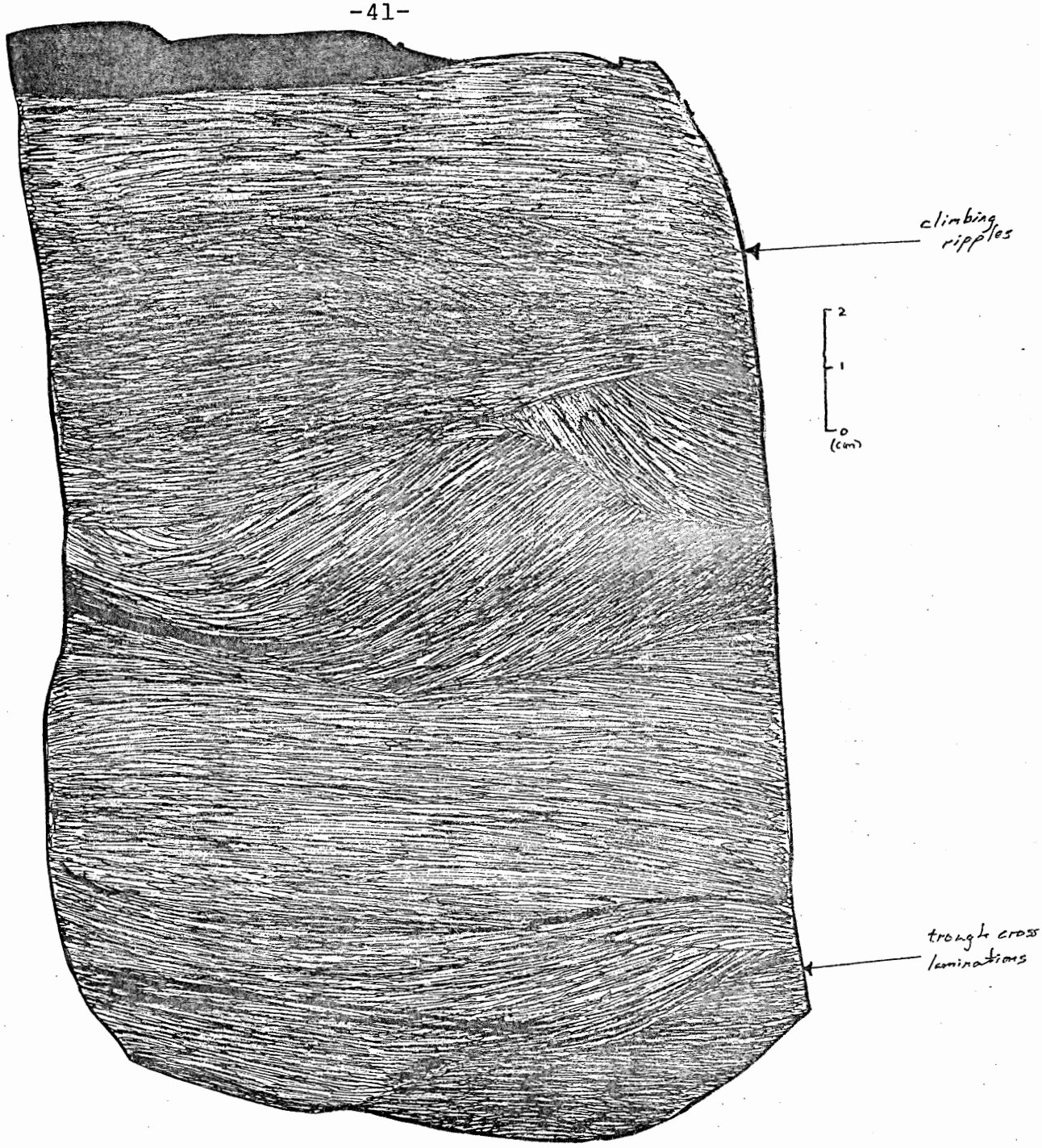

Figure 6: A sketch of a polished slab, facies C. Sedimentary structures are noted around the diagram.

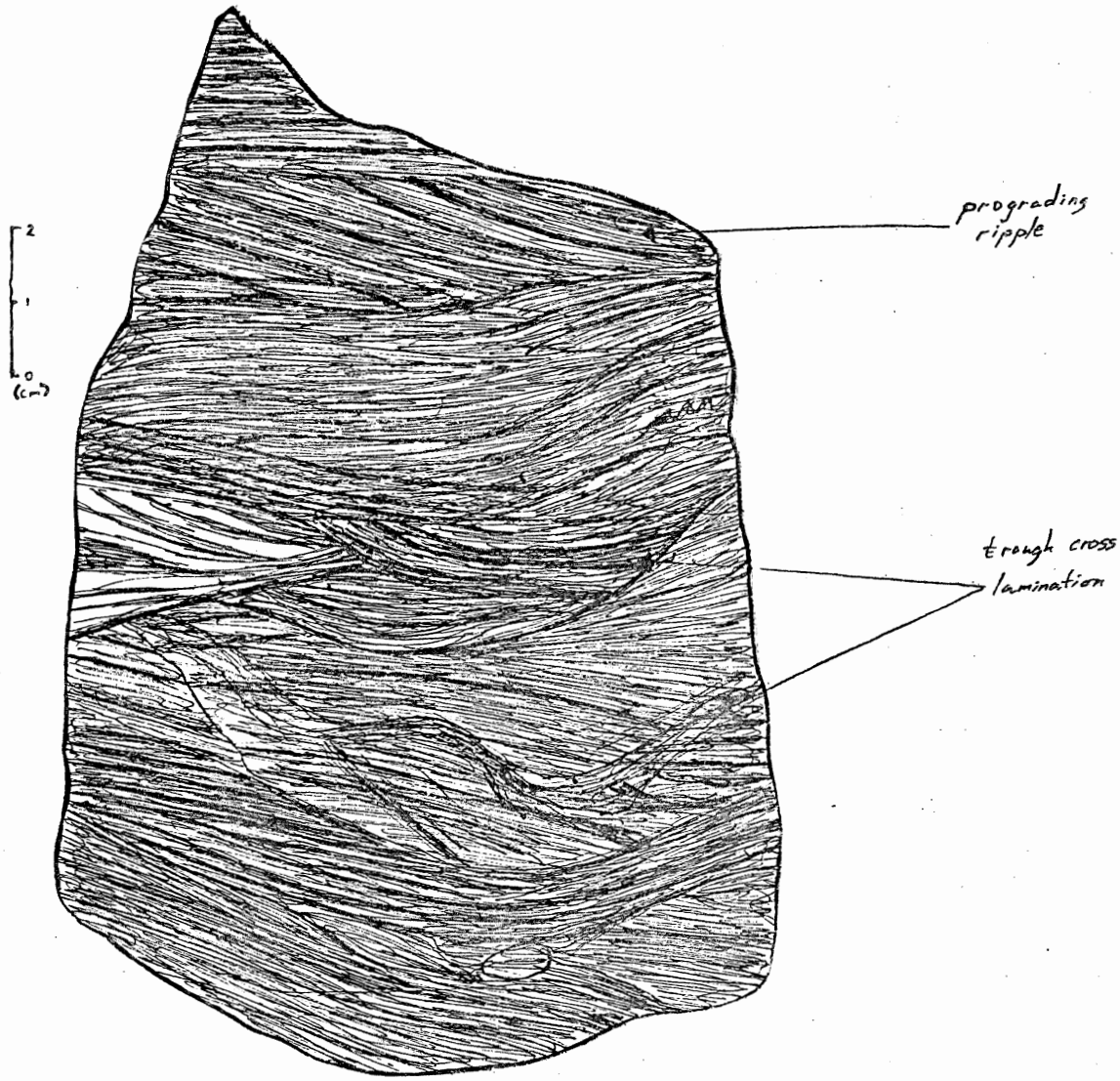

Figure 7: A sketch of a polished slab, facies C. Sedimentary structures are noted around the diagram.

lenticles represent:

1. starved ripples, which developed during episodes of sediment starvation;

2. incomplete boudinage structures.

Associated with the lenticles are bulbous aggradations of silt in what are mainly planar beds (see Plate 9 for an illustration). The bulbous aggradations of silt are climbing ripples.

(viii) Sole Marks: Sole marks are scarce due to the lack of good exposure of bedding planes. The sole marks are limited to current scours such as flute marks; which consist of discontinuous elongate bulbosities (Plate 6a). The flute marks are only observed in facies D.

(ix) Load Structures: Load structures consist of sand bulging into underlying mudstone or grainstone beds. They are more bulbous than flutes and are associated with facies C and D.

(x) Fine, Parallel Laminations: Distinct, fine parallel laminations are seen in outcrop exposures of facies D. The parallel laminations and grain size become finer up section. An examination of a polished section indicates that the parallel laminations in facies D develop from wavy laminations (figure 5); this suggests that the parallel laminations of facies D develop as a result of a decrease in the flow power.

(xi) Bedding Planes: Bedding planes are predominantly planar; some are wavy. Wavy bedding planes have an amplitude between one and five centimetres, the norm being approximately two centimetres. Plates 4a and 4b illustrate wavy bedding planes with

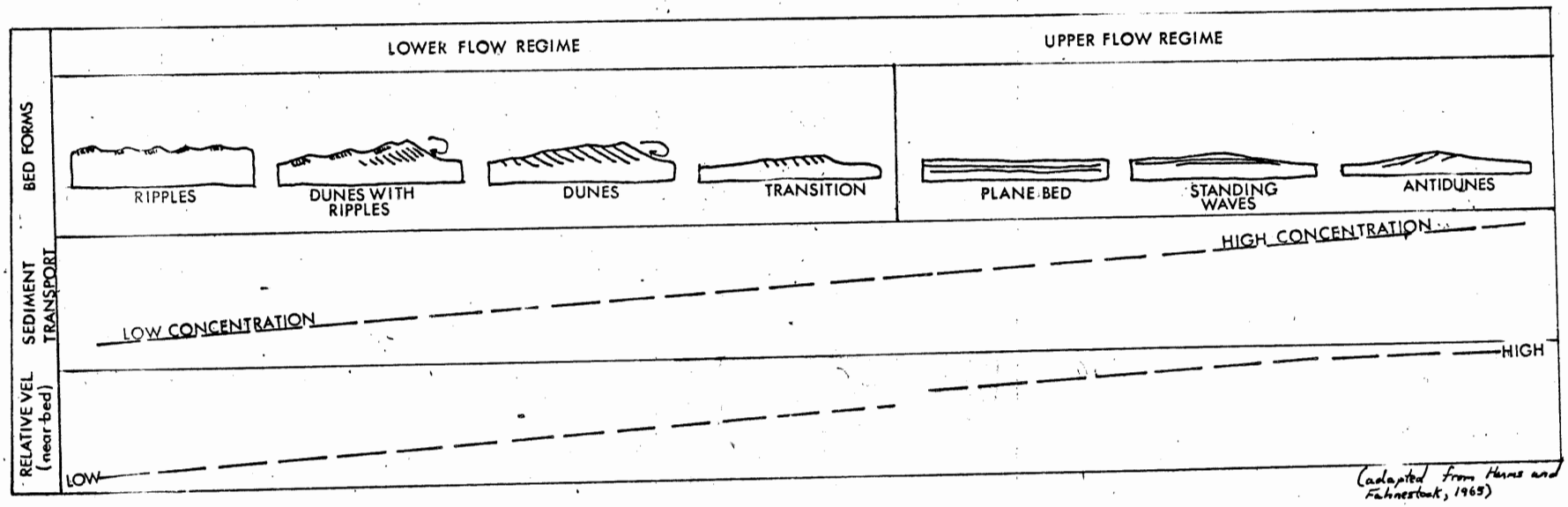

Figure 8: A diagram of the flow regimes of sand size sediment and two of their characteristics. Rippled bed and plane beds have been seen in the fine sandstone and siltstone units at Ovens Park. Flow regimes that may be analgous to the flow regimes in sand size sediment may be responsible for the formation of these bed forms. In the text, these bed forms are described as developing under high power flow and low power flow conditions; high power flows develop plane bed forms, low power flows develop rippled bed forms; low power flows can only transport sediments in low concentration and have relatively slow velocities; high power flows transport high sediment concentration and can transport larger grains of sediment at high velocities.

amplitudes of one to five centimetres . Wavy bedding planes were observed in subfacies C_2, D_2, and F_2. These wavy bedding planes form as a result of aggradation of silt; the aggradation of silt forms climbing ripples (Harms et al, 1975). Figure 8 shows the various types of bedding planes that are associated with upper and lower flow regimes and sand particles. Strata that is composed of silt particles is known to have bedforms similiar to the bedforms in Figure 8 and the power of the depositing flow that is associated with the bedforms in Figure 8 is assumed to have a counterpart depositing flow that would develop bedforms similar to those of Figure 8 in silt sediments.

Boudins form when preexisting bodies that are more competent than the surrounding rock are segmented (Hobbs, Means, and Williams, 1976). During the formation of boudinage, a body, such as a given bed, is broken up into a series of elongate bodies aligned parallel to each other. The boudins are separated by material that originally lay on either side of the boudinage layer. Incomplete boudinage forms where preexisting bodies have necked but not broken through. Boudins are commonly aligned parallel to the axes of folds.

Hobbs, Means, and Williams (1976) state that boudins are commonly large in size and are restricted to certain surfaces in a deformed sequence.

Detailed examination of internal structures indicates that wavy bedding planes develop as true sedimentary features. Climbing ripples are the sedimentary structures that develop the wavy bedding planes.

SECTION IV - Facies Interpretation and Sequence Anaylsis

Facies Interpretation

Facies A - Facies A is a massive positive and reverse graded very fine sandstone-coarse siltstone unit. The fine siltstone- mudstone rip up intraclasts (Plate 1b) suggest that this facies developed in a high power regime. It is the coarsest facies and it lacks internal layering. Facies A characteristics are similar to the Bouma A division characteristics.

Piper (1973) commented that poorly sorted silts lacking good grading, laminations and containing dispersed mud and silt clasts are features hard to explain by steady tractional bed load deposition; he suggests unsteady flow near the head of the turbidity current and tractional bed load movement in the tail of a turbidity current as a depositional process for a silt equivalent of a Bouma A division (i.e., Facies A).

Facies B - Facies B is a very fine sandstone - coarse siltstone unit with parallel laminations. It is generally thinner than units of Facies A. Facies B is similar to the Bouma B division; it may represent a high power regime.

Facies C - Facies C is an intermixed coarse siltstone and medium siltstone with cross laminations derived from current ripples. It is thinner than Facies A and B and it is similar to the Bouma C division. The presence of climbing ripples suggests that in this facies the rate of

deposition of sediment is decreasing less rapidly with time than the rate of bedload transport; the climbing ripples are good evidence of deposition by turbidity currents (Piper, personal communication, 1981). The relationship in Facies C of one cross laminated set to another cross laminated set changes from erosional in the lower part of the facies to gradational in the upper part. Cross laminations often develop symmetrical undulations that form the undulose bedding planes of subfacies C_2 (Plate 3b).

Subfacies C_1 units occur most frequently above facies B units; subfacies C_1 and subfacies C_2 record rapid sediment accumulation from a moderate to low power regime.

Facies D - Facies D consists of medium to fine siltstone with interbedded mudstone. Climbing ripples and wavy laminations grading upwards into fine, parallel laminations suggests that facies D develops from a decreasingly low power regime. Convolute laminations and flute marks associated with this facies suggests that it was deposited rapidly. Grain size analysis of the flute marks associated with this facies indicates flow velocities of 8-12 cm/sec (Figure 9, Appendix 3a).

Facies E - Facies E consists of clayey siltstones, and silty mudstones with thin, interbedded coarse to medium siltstone. Subfacies E_1 consists of mudstones interbedded

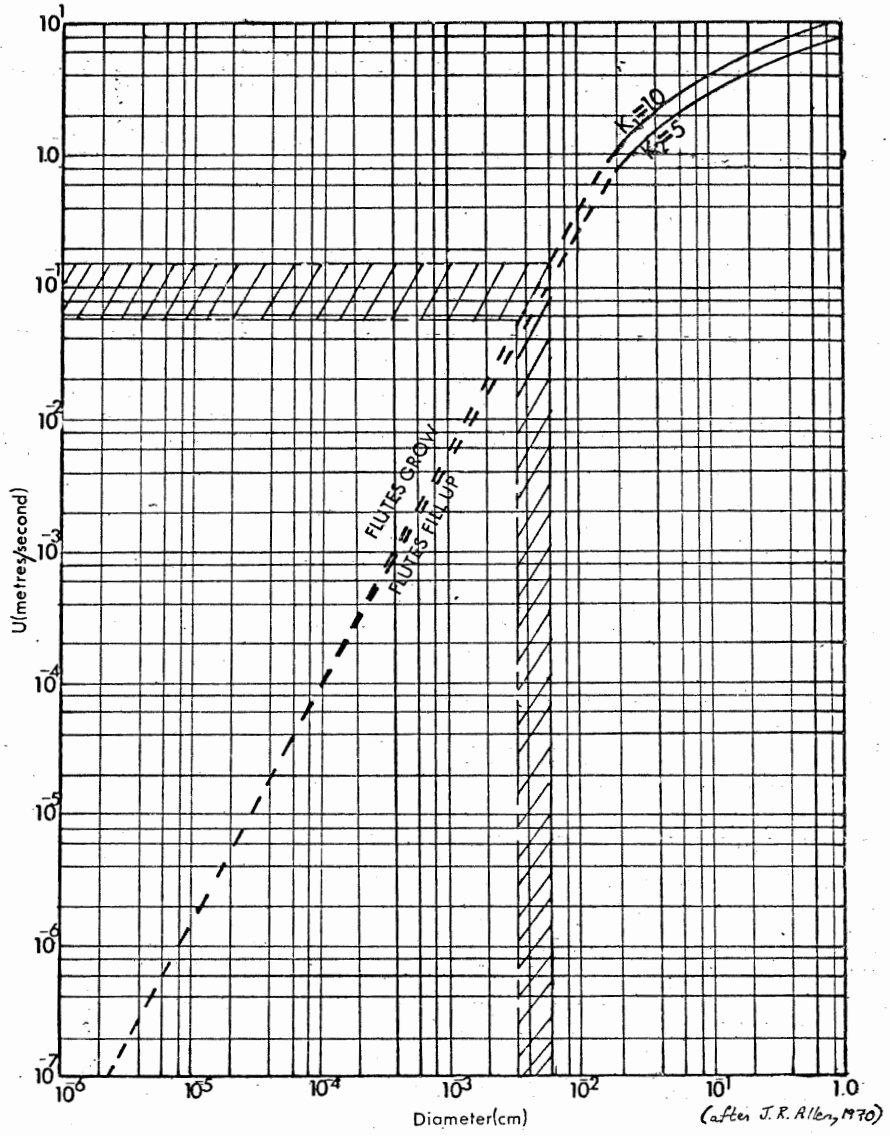

Figure 9: Theoretical criterion for the growth of flute marks with respect to quartz grain size diameters. The dashed line represents an extrapolation of experimental data. The cross hatched zone represents the grain size range of quartz grains in a flute mark found at Thunder Cave. The grain size analysis is presented in graphical form in figure 15, Appendix 3.

with thin, regular coarse to medium siltstone. Stow and Shanmugam (1980) suggest a low flow regime where thin, regular coarse to medium siltstone is interbedded with thick shale units. Subfacies E_1 corresponds to their T_3-T_4 divisions which, they suggest, could be found close to channels and on fan lobes. Hesse and Chough (1980), describe a Recent, parallel laminated turbidite mud unit that is similar in character to facies D fining up to subfacies E_1. This Recent parallel laminated mud originated from channel levee deposits.

Subfacies E_2 consists of shale with thin, interbedded, lenticular and wavy, medium to coarse siltstone beds. This facies corresponds to the T_1-T_2 divisions of Stow and Shanmugam (1980) and facies division E_1 of Piper (1978). Stow and Shanmugam (1980) suggest that the divisions T_1 and T_2 represent a low flow regime.

Subfacies E_3 is primarily homogeneous, wavy, fine siltstone and mudstone. It is analgous to Stow and Shanmugam (1980) T_5-T_7 divisions and divisions E_3 and E_2 of Piper (1978). Stow and Shanmugam (1980) state that their T_5-T_7 units are dominant away from the channel axes. They suggest that divisions T_5-T_7 would be found on levees, in interchannel areas, on the outer fans and in abyssal plain environments. Piper (1978) indicates that his E_2 and E_3 divisions are common in deep sea fan valleys and on the low parts of deep sea fans.

Section one (Appendix 1) has two distinct facies assemblages one encompassing the strata on the base

(21.50 - 14.0 metres) and the top (10.5-0.0 metres) of the measured section and one that encompasses strata in the centre (14.0 - 10.0 m) of the section. The strata in the centre of the section have characteristics of Bouma Ta, Tb, and Tc divisions. The strata encompassing the part of the section overlying and underlying the central part of the measured section have characteristics of Bouma T_c, Td, Te, divisions. The section strata from 10.5 - 7.5 metres has characteristics of Bouma T_c-Td-Te divisions, mostly Tc-Te. Walker (1979) suggests that sediments consisting of silt and clay and that produce Tc-Te beds could indicate levee or back-levee environments. Mutti (1977) identified two types of levee facies: one of interbedded sandstone and mudstone (this is similar to facies D) that is deposited on the levee face that slopes towards the channel axis, and a second similar mudstone facies with very thin beds of sandstone and siltstone (similar to subfacies E_1) that is deposited on the levee crest and the levee face that slopes towards adjacent interchannel depressions. It is proposed, by analogy, facies A, B, and subfacies C represent distributary channel facies while facies D and subfacies E_1 would respectively represent levee and back-levee deposits.

A study of Navy Fan by Normark, Piper and Hess (1979) indicates that two assemblages of current patterns exist on deep sea fans. One assemblage is confined to distributary channels and the other assemblage develops in the levee, back-levee, and interchannel areas of the deep-sea fans. Figure 10 shows that the paleocurrent

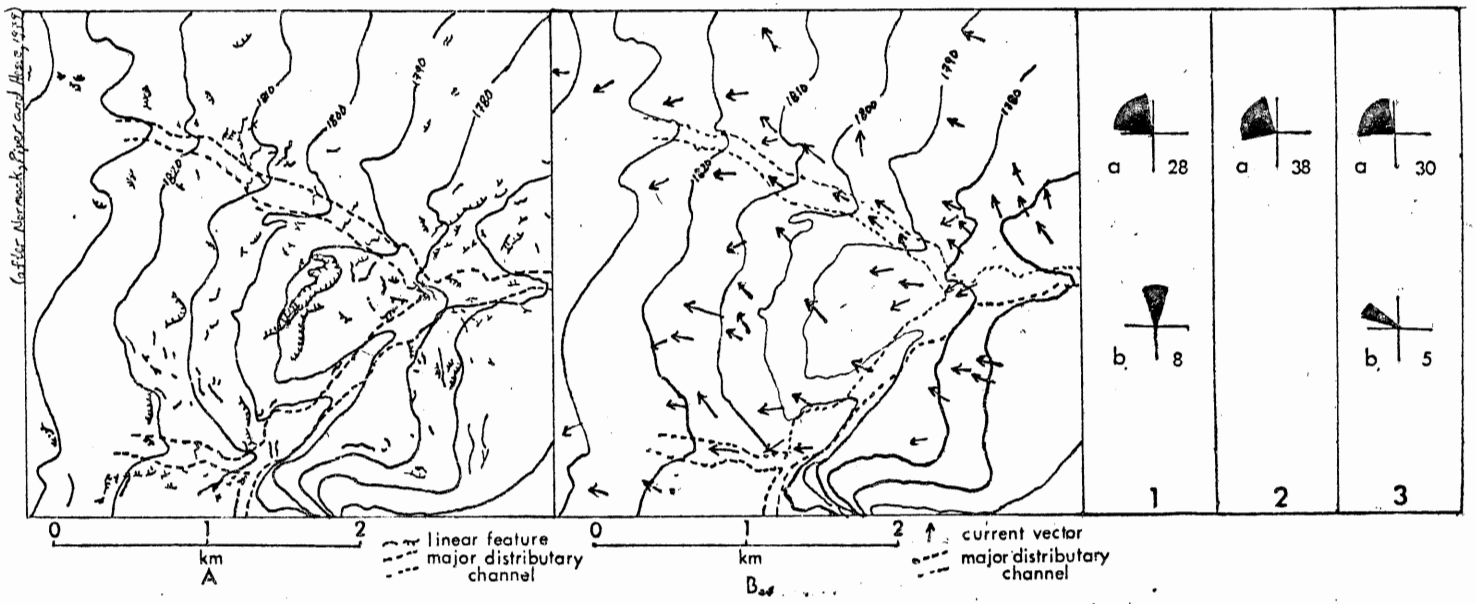

Figure 10: Paleocurrent trends at Ovens Park compared to current trends at Navy Fan. Diagram A shows the relative distribution of flute marks on a portion of Navy Fan; diagram B indicates the direction of flow on this portion of Navy Fan, using the flute marks as paleocurrent indicators. Diagram 1a shows the range of paleocurrent directions in the top and bottom portions of the Thunder Cave section; diagram 1b shows the range of directions for the middle portion of the section at Thunder Cave. Diagram 2a illustrates the paleocurrent vector directions at Ovens Park Beach. Diagram 3a illustrates the range of vector directions in the interchannel areas at Navy Fan; diagram 3b illustrates the range of paleocurren vector directions within the distributary valleys at Navy Fan.

assemblage that is derived from distributary channels are in a northwesterly direction and have a narrow range of distribution. The vectors that represent the levee, back levee, and interchannel areas span a west to north direction and have a wide range of distribution (figure 10; 3a). The paleocurrents assemblage in the central portion of the Thunder Cave section (section one, Appendix 1) has a northern direction with a narrow range of distribution (Figure 10;1b); the base and top portions of the section have paleocurrent vector assemblages that indicate a flow direction towards the northwest, these vectors show a wide range of distribution (figure 10;1a). The paleocurrent vector assemblages in Figure 10;1b, 3b, may indicate a facies assemblage that has restricted flow directions, while the vector assemblages of Figure 10;1a, 2a and 3a indicate a facies assemblage that has a relatively "open" flow direction, i.e., the only restricting condition on the flow direction is the direction of the slope of the topography. Restricted flow conditions exist in the distributary channels of deep-sea fans; "open" flow conditions exist in the levee, back-levee, and interchannel areas of deep sea fans. The central portion of section one (Appendix 1) may represent a distributary channel facies assemblage and the base and top portions of section one may represent a levee, back-levee, and interchannel areas of a deep-sea fan.

In section two (Appendix 2) the paleocurrent vectors

have a northwest direction with a wide range of distribution (figure 11,2a). This may indicate that section two is composed of levee, back-levee, and interchannel sediments.

Stow and Shanmugam (1980) suggest that contourites should show a distinct paleocurrent trend with a narrow range of distribution. This is not the case at Ovens Park and The facies descriptions and paleocurrent trends of the sections measured at Ovens Park would suggest that the strata at Ovens Park were deposited by turbidity flows. The thin layering of strata indicates low sediment concentrations and a grain size analysis of a flute mark suggests a relatively slow velocity for the turbidity flow (figure 9). Waning current velocites during the passage of a single flow would develop the observed bedding plane features.

Facies Sequence Analysis

After defining nine facies and subfacies the problem remains of analyzing their sequence and distilling the sequence into a generalized form that can be used as a basis for a facies model.

Two ways in which facies relationships and sequences can be interpreted are:

1. By a "Facies Relationship Diagram".

2. By tallying facies transitions and converting into probabilities. A Markov chain analysis can be performed on the probabilities. These probabilities are organized into matrices.

Analytical Method

The method used in this thesis is an analytical method devised to analyze for facies successions. Four "steps" for analytical transitions were performed to distil the most probable sequence of facies in the sequence. The information described below is derived from Harbaugh and Bonham-Carter (1970).

The analysis is a simple first-order Markov chain analysis. This analysis depends only on single steps, it analyzes for the relationship between a given bed and the next bed immediately succeeding it. The first step is referred to as a tally matrix or a transition count matrix. It tabulates the number of times that all possible vertical facies transitions occur in a given stratigraphic succession. The row number denotes the lower bed of each transition couplet. The upper bed is denoted by the column number. Elements of the transition count matrix are referred to by the symbol fij., where i = row number and j = column number. Where i = j, transitions have only been recorded where the facies shows a change in character.

Probability matrices are derived from the transition count matrix. One matrix represents the probability of a given transition occurring randomly. Given any state i , the probability of this state being succeeded by any other state j is dependent only on the relative proportions of the various states present. Thus:

$$rij = sj/(t-si)$$

t = total number of beds = fij,

sj = the sum of fij for the jth column of the f matrix

si = the sum of fij for the ith row of the f matrix

In the method outlined above i = j transitions are not permitted, thus the total range of possibilities must be set to exclude them. This component must be subtracted from the equation.

The second matrix containing element pij gives the probabilities of a given transition occurring in a given section.

$$pij = fij/si$$

The value of a p matrix row sums to one and thus reflects a Markovian relationship.

A difference matrix is constructed in which

$$dij = pij - rij$$

Positive entries in the d matrix serve to emphasize the Markov property by indicating which transitions have occurred more frequently than random frequency.

To test the significance of the differences between the p matrix and the r matrix a chi-squared test is performed. The statistical test for the Markov property as described by Harbough and Bonham-Carter (1970) distinguishes between the idea that successive events are independent of each other or the events are not independent. If the events are dependent on each other they may form a first order Markov

chain. The expression is:

$$-2 \ln \lambda = 2 \sum_{i,j}^{m} fij \quad \ln \left(\frac{pij}{pj}\right)$$

pij = probability in cell i j of matrix

pj = probabilities for the jth column ($=pij = \sum_{i}^{m} fij / \sum_{i,j}^{m} fij$)

mij = transition frequency total in cell ijj of the tally matrix

m = total number of states

The number of degrees of freedom = $(m-1)^2$

The null hypothesis is that the vertical succession of strata was derived by random variation in the depositional mechanism.

Facies Sequence Interpretation

This section is devoted to the interpretation of the facies sequence and presenting the facies relationships as a local model.

Thunder Cave - Section One (Appendix One). (Refer to figure 11 for a diagrammatic presentation of the facies sequence).

The close association between facies A, B, and subfacies C_1, and the negligible probability of a facies A or B transition to facies D , E, or subfacies C_2 (see figure 11b) suggests that the mechanism of deposition of facies A and B is not the same as the mechanism for the deposition of facies D, E and subfacies C_2. The mechanism for the deposition of subfacies C_1 is related to the mechanism for the deposition of facies A and B; since there is an association between subfacies C_1 and subfacies E_1 a depositional relationship must exist between these two subfacies.

The massive character of facies A and the coarse, parallel laminated character of facies B are characteristics similar to the Bouma A and B divisions of sand turbidites. Bouma A and B divisions are interpreted to have been deposited under upper flow regime conditions (Walker,1979; figure 8). Upper flow regime conditions include high velocity flows and high sediment concentrations. These conditions, with respect to the flow regime, are outlined in figure 8 . At Thunder Cave, a small ($\approx$15 centimetres deep) channel was observed and documented (Section One,

Tally Matrix

Upper Unit

Lower Unit	A	B	C_1	C_2	D_1	D_2	E_1	E_2	E_3	S_i	$(T-S_i)$
A	0	12	3	0	0	0	0	0	0	15	159
B	8	0	8	2	0	2	3	2	0	25	149
C_1	3	5	0	0	1	1	7	1	2	20	154
C_2	0	3	0	0	4	1	1	1	3	13	161
D_1	0	0	0	2	0	4	6	4	2	18	156
D_2	0	1	0	4	6	0	7	4	1	23	151
E_1	3	1	4	3	9	8	0	2	2	32	142
E_2	0	0	1	2	1	5	4	0	2	15	159
E_3	2	1	3	3	2	1	0	1	0	13	161
S_j	16	23	19	16	23	22	28	15	12	T=174	

Transition Probability Matrix

	A	B	C_1	C_2	D_1	D_2	E_1	E_2	E_3
A	0	.8	.2	0	0	0	0	0	0
B	.32	0	.32	08	0	.08	.12	.08	0
C_1	.15	.25	0	0	.05	.05	.35	.05	.10
C_2	0	23	0	0	.31	.08	.08	.08	.23
D_1	0	0	0	.11	0	.22	.33	.22	.11
D_2	0	.04	0	.17	.26	0	.32	.17	.04
E_1	.09	.03	.13	.09	.28	.25	0	.06	.06
E_2	0	0	.06	.13	.06	.33	.27	0	.13
E_3	.15	.08	.23	.23	.15	.03	0	.08	0

$= P_{ij}$

Independent Trials Probability Matrix

	A	B	C	C_2	D_1	D_2	E_1	E_2	E_3
A	0	.14	.12	.10	.14	.14	.18	.10	.08
B	.11	0	.13	.11	.15	.15	.18	.10	.08
C	.10	.15	0	.10	.15	.14	.18	.10	.08
C_2	.11	.16	.12	0	.14	.14	.17	.10	.07
D_1	.10	.15	.12	.10	0	.14	.18	.10	.08
D_2	.12	.16	.13	.11	.16	0	.14	.10	.08
E_1	.11	.16	.11	.11	.16	.16	0	.12	.08
E_2	.10	.14	.12	.10	.14	.13	.18	0	.07
E_3	.10	.13	.12	.10	.14	.14	.18	.09	0

$= r_{ij}$

Difference Matrix

	A	B	C_1	C_2	D_1	D_2	E_1	E_2	E_3
A	0	.66	.08	-10	-14	-14	-18	-10	-08
B	.21	0	19	-03	-15	-06	-06	02	-08
C_1	.05	10	0	-10	-10	-09	.17	-05	.02
C_2	-11	.07	-12	0	.17	-06	-09	-02	.16
D_1	-10	-16	-13	.01	0	.08	.15	.12	.03
D_2	-12	-12	-13	.06	.10	0	.18	.07	-04
E_1	-02	-13	.02	-02	.12	.09	0	-04	-02
E_2	-10	-14	-06	.03	-08	.20	.09	0	06
E_3	.05	-05	.11	13	.01	-06	-18	-01	0

$= d_{ij}$

$d.o.f = 64$

$-2\log_e \lambda = 202.973$

$\chi^2 = 83.635$

χ^2 value is derived from Table IV. Distribution of χ^2 (Fisher and Yates, 1963)

Since $-2 \ln \lambda$ is much greater than the χ^2 value, the null hypothesis can be rejected.

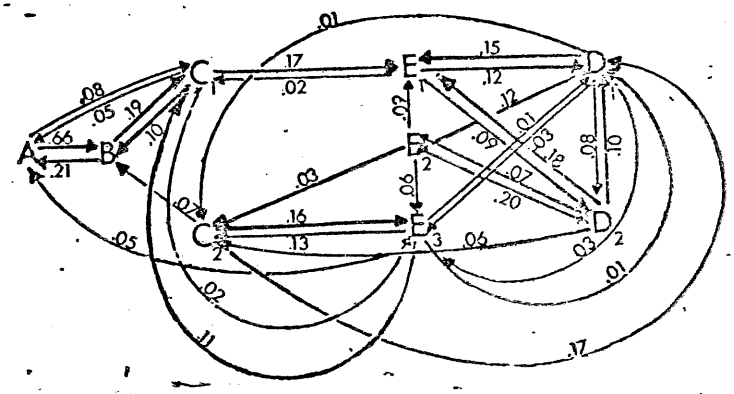

Figure 11a: Facies relationship diagram showing the transitions that occur more commonly than random. This facies relationship model represents a section measured at Thunder Cave.

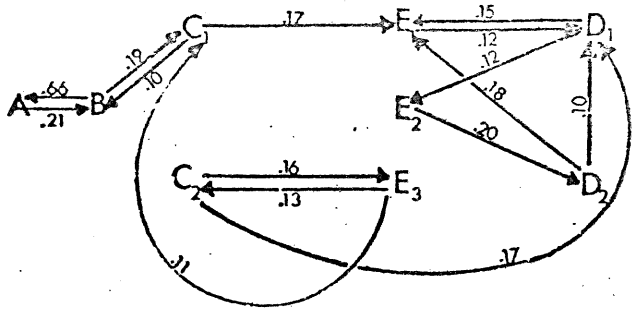

Figure 11b: Simplified facies relationship diagram showing the transitions that occur most commonly (> + .10). This facies relationship model represents section measured at Thunder Cave.

Appendix 1), near the base of the section; this channel was filled with sediments that had the characteristics of facies A and B. Nelson (1975) stated that Bouma (1962) Tab units are deposited in middle and lower fan valleys. Using the data of Nelson (1975) and the observation of the small channel filled with facies A and B divisions, the facies A and B divisions are interpreted as deep sea fan valley - distributory channel deposits and to have been deposited under high flow power conditions. Subfacies C_1 with its plane bedding and climbing ripples, probably represents a unit that was deposited under lower flow conditions than facies A and B. The presence of planar bedding and the lack of significant (<5%) amounts of mudstone suggests that there was sufficient turbulence in the turbidity flow to keep the fine silt and mud particles suspended but insufficient turbulence to prevent the development of climbing ripples. The association of subfacies C_1 with facies B suggests that the decrease in flow power takes place within the channel rather than outside the channel but the association of subfacies C_1 with subfacies E_1 suggests that subfacies C_1 is deposited outside the fan valley - distributary channels. Facies C_1 is interpreted to be an inter-intrachannel facies.

The sequence of transitions

$$E_1 \longrightarrow D_1 \longrightarrow E_2 \longrightarrow D_2$$

observed in Figure 11b suggests that

an upward decrease in flow power occurs. Subfacies E_1 and D_1 develop when the flow power is sufficient to produce plane beds; subfacies E_2 and D_2 develop when the flow power is too low to develop plane beds but sufficient to develop wavy, undulose bedding planes. Subfacies E_2 and D_2 may represent a distal extensions of subfacies E_1 and D_1 respectively; subfacies E_2 and D_2 develop when the turbidity flow has lost so much flow power that it produces wavy, undulose bedding planes. Possible depositional sites for subfacies E_1 and D_1 would be on channel levees and depositional sites for subfacies E_2 and D_2 would be back-levee and interchannel areas. Schenk and Harris (1975) suggested that strata of the Halifax Formation at Black Rock Beach that have characteristics of subfacies E_2 and D_2, were deposited as overbank turbidites (?).

Subfacies C_2 has a high probability of a transition to subfacies E_3 and subfacies D_1. The wavy undulose bedding planes and the high percentage (>5%) of mudstone in the grainstone fabric suggest that subfacies C_2 was deposited by a turbidity flow with low flow power. The presence of climbing grainstone ripples and the high proportion of grainstone (>90%) in this facies suggests that this subfacies may be related to subfacies C_1. The transition of subfacies C_2 to subfacies D_1 suggests that the flow power of subfacies C_2 is higher than the flow power of subfacies D_1.

A plausible explanation of this phenomenon would have subfacies C_2 requiring a higher flow power to transport its coarse bed load than subfacies D_1, which has a finer grain fabric than subfacies C_2. When the coarse sediments in the turbidity current have been deposited as subfacies C_2, the flow power may be sufficient to develop plane beds in the fine grain sediments that are associated with subfacies D_1. The high probability of subfacies C_2 transcending to subfacies E_3 may be the result of an insufficient supply of fine grainstone sediment (in the turbidity flow) that would produce grainstone beds that are characteristic of facies D or subfacies E_1 and E_2. Possible depositional sites for subfacies C_2 would be similar to subfacies C_1, but a higher proportion of subfacies C_2 would be found in the interchannel areas of deep-sea fans since this would be the most probable realm of low power turbidity currents. The relationship of subfacies C_1 with subfacies D_1 suggests the existence of subfacies C_1 in or near a distributary channel. Thus, subfacies C_2 can be considered an intra-interchannel facies. Subfacies E_3 is either an end of flow facies or a hemipelagic facies.

Ovens Park Beach - Section Two (Appendix 2). (Refer to Figure 12 for a diagrammatic presentation of this facies sequence.)

The facies relationship and characteristics in this section are basically similar to the facies relationships in the section measured at Thunder Cave.

Tally Matrix

Upper Unit

Lower Unit	A	B	C_1	C_2	D_1	D_2	E_1	E_2	E_3	S_i	$(T-S_i)$
A	0	0	0	0	0	0	0	0	0	0	174
B	0	0	0	0	0	0	0	0	0	0	174
C_1	0	0	0	0	0	0	1	1	0	2	172
C_2	0	0	0	0	1	5	0	28	4	38	136
D_1	0	0	1	0	0	0	1	5	3	10	164
D_2	0	0	0	3	0	0	2	28	4	37	137
E_1	0	0	0	1	0	2	0	2	1	6	168
E_2	0	0	1	30	4	28	2	0	2	67	107
E_3	0	0	0	6	5	2	0	1	0	14	160
S_j	16	23	19	16	23	22	28	15	12	T=174	

Transition Probability Matrix

	A	B	C_1	C_2	D_1	D_2	E_1	E_2	E_3
A	0	0	0	0	0	0	0	0	0
B	0	0	0	0	0	0	0	0	0
C_1	0	0	0	0	0	0	.5	.5	0
C_2	0	0	0	0	.02	.13	0	.74	.11
D_1	0	0	.1	0	0	0	.1	.5	.3
D_2	0	0	0	.08	0	0	.05	.76	.11
E_1	0	0	0	.17	.0	.33	0	.33	.17
E_2	0	0	.02	.45	.06	.41	.03	0	.03
E_3	0	0	0	.43	.36	.14	0	.07	0

$= P_{ij}$

Independent Trials Probability Matrix

	A	B	C_1	C_2	D_1	D_2	E_1	E_2	E_3
A	0	0	0	0	0	0	0	0	0
B	0	0	0	0	0	0	0	0	0
C_1	0	0	0	.23	.06	.22	.04	.38	.23
C_2	0	0	.02	0	.07	.27	.04	.48	.10
D_1	0	0	.01	.24	0	.23	.04	.40	.09
D_2	0	0	.01	.29	.07	0	.04	.48	.10
E_1	0	0	.01	.24	.06	.22	0	.39	.08
E_2	0	.0	.02	.37	.08	.35	.06	0	.13
E_3	0	0	.01	.25	.06	.23	.04	.41	0

$= r_{ij}$

Difference Matrix

	A	B	C_1	C_2	D_1	D_2	E_1	E_2	E_3
A	0	0	0	0	0	0	0	0	0
B	0	0	0	0	0	0	0	0	0
C_1	0	0	0	-.23	-.05	-.22	.46	.12	-.08
C_2	0	0	-.02	0	-.04	-.14	-.04	.25	-.01
D_1	0	0	.09	-.24	0	-.23	.07	.10	.21
D_2	0	0	-.01	-.21	-.07	0	.01	.27	.01
E_1	0	0	-.02	-.07	-.07	.11	0	-.06	.11
E_2	0	0	0	.08	-.02	.06	-.03	0	-.10
E_3	0	0	-.01	.18	.30	-.09	-.04	-.34	0

$= d_{ij}$

dof = 64

$-2\log_e \lambda = 214.808$

$\chi^2 = 83.635$

Since $-2 \ln \lambda$ is much greater than χ^2 value, the null hypothesis can be rejected.

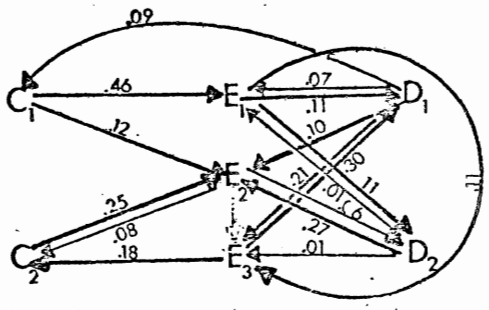

Figure 12a: Facies Relationship diagram showing the transitions that occur more commonly than random. This facies relationship model represents a section measured at Ovens Park Beach.

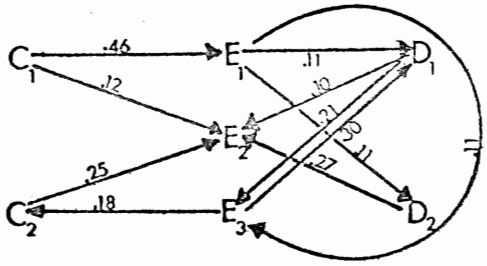

Figure 12b: Facies Relationship diagram showing the transitions that occur most commonly (> + .10): This facies relationship model represents a section measured at Ovens Park Beach.

χ^2 value is derived from Table IV. Distribution of χ^2 (Fisher and Yates, 1963)

In this section, the high probability of the transition of subfacies C_1 to E_2, D_2 to E_2, and C_2 to E_2 (Figure 12b) suggests that:

1. A loss of turbulence prevents grainstone sediments from being suspended.

2. Grainstone sediment starvation has occurred; (there is no longer enough grainstone remaining in turbulent suspension), the lack of grainstone prevents the development of wavy bedding that is a characteristic of subfacies D_2 and E_2; there may be sufficient grainstone sediment available to form the lenticles that are characteristic of subfacies E_2.

The high probability of transitions from subfacies E_1 to E_3, and D_1 to E_3, can be explained by suggesting processes similar to those that occurred in the subfacies C_1 to E_2, D_2 to E_2, and C_2 to E_2 transitions, namely: 1. loss of turbulence, and 2. grainstone sediment starvation.

The transition of subfacies E_1 to D_2 probably suggests a decrease in flow power of the turbidity current and the transition of subfacies C_1 to E_1 can be explained as a process similar to that which occurred at Thunder Cave. The upward transitions of subfacies $E_3 \longrightarrow C_2$, and $E_3 \longrightarrow D_1$, (Figure 12b), probably represents the deposition of a new turbidity deposit on the "end of the flow" deposit (subfacies E_3).

The most probable area for the deposition of the strata associated with the section at Ovens Park Beach would be the mid-fan region of the deep-sea fan. The most probable area for the deposition of the strata at Thunder Cave would be a distributary

channel, levee, back-levee region in the midfan area of a deep sea fan.

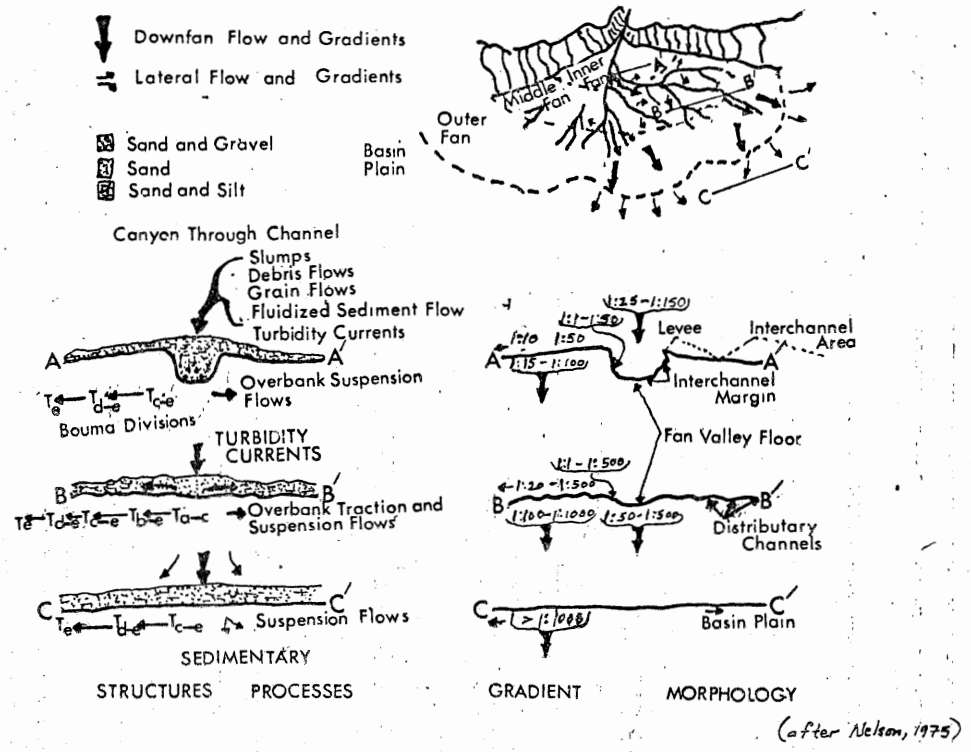

Figure 13: An illustration of the various features of a deep sea fan. In section B-B, Bouma Ta and Tb units are found in the distributary channel; Tc-Te units are found near the channel as over bank deposits. Bouma equivalent facies A, B, and C are found at Thunder Cave. Strata with no Bouma Ta or Tb equivalents, but with Bouma Tc, Td and Te equivalents are found at Ovens Park Beach.

SECTION V-CONCLUSIONS

Conclusions

1. The strata at Ovens Park are composed of very fine sandstone, siltstone and mudstone.

2. Sedimentary structures and the similarity of facies A, B, and C to Bouma Ta, Tb, and Tc divisions respectively suggest that these units were deposited by turbidity flows. The sedimentary structures observed in facies D and E suggest that these units were deposited by turbidity flows.

3. The fining-up sequence in the strata at Thunder Cave suggests these strata were deposited by turbidity flows.

4. Two distinct types of bed forms were distinguished at the Ovens Park study area:a)wavy and lenticular beds,b)plane beds. Plane beds are associated with divisions of the Bouma sequence with upper flow regime characteristics(Ta,Tb); wavy and lenticular bedforms are found only in divisions of the Bouma sequence that have lower flow regime characteristics (Tc, Td, and Te). Plane beds are associated with facies A and B. Wavy and lenticular beds are associated with facies C, D, and E. Thus facies A and B form under high power flow conditions while facies C and D may form under high or lew flow power conditions.Plane bedding may indicate the proximity of a facies unit to the

source of the turbidity flow, wavy and lenticular beds may develop as a result of waning velocities and decreasing turbulence in a turbidity flow.(Refer to Figure 14 for an illustration).

5. Lenticular beds develop through a process of grainstone sediment starvation and grainstone aggregation in a moderately turbulent turbidity flow.

6. Facies A, B and subfacies C_1 occur in close mutual association. The sedimentary structures observed in the units suggest that the depositional mechanism had a higher flow power relative to the depositional mechanism that deposited facies D, E, and subfacies C_2.

7. Facies D has characteristics similar to the characteristics of the Bouma Tc and Td divisions. Subfacies E_1 and E_2 have characteristics similar to division E_1 of Piper (1978) and and division T_1 to T_6 of Stow and Shanmugam (1980). Divisions E_2 and E_3 of Piper (1978) and divisions T_6 and T_7 of Stow and Shanmugam (1980) have characteristics similar to subfacies E_2. Subfacies E_3 has characteristics similar to division F of Piper (1980) and division T_8 of Stow and Shanmugam (1980).

8. The data of Appendix 3 suggest a coarsening-up trend in the higher flow power units (facies A and B) and a fining up trend in the lower flow power deposits (facies C, D, and F).

9. Facies A and B are probably associated with distributary channels (Figure 13). Subfacies C_1 is an inter-intrachannel

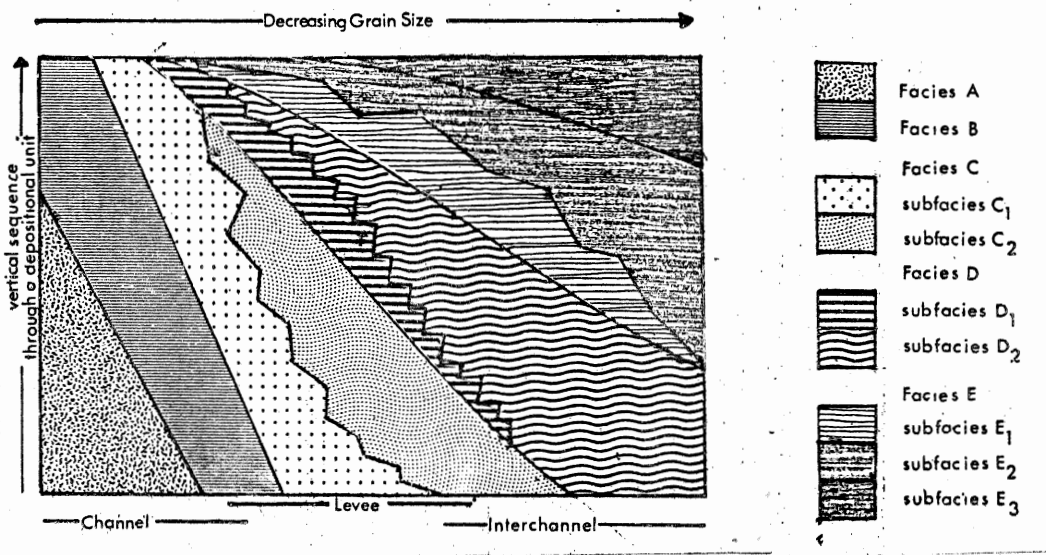

Figure 14: A Facies Model Diagram illustrating the facies relationship and the factors affecting their distribution and characters. At the bottom of the diagram, possible depositional sites for the facies units are noted.

facies while facies D and E represent levee, back-levee, and interchannel facies within the strata at Ovens Park. Subfacies C_2, D_2, and E_2 may represent: a) distal turbidties correlatives of subfacies C_1, D_1, and E_1, b) sediment deposits that were deposited under waning flow power conditions.

Information derived from Nelson (1975) (Figure 13) suggests that the strata at Ovens Park were deposited in the middle fan region of a deep sea fan.

10. The Halifax Formation probably represents a "distal" turbidite member of the Meguma Group. The quartz grain type, and the sediment size and paleocurrent directions suggest that the Halifax Formation represents a "distal" component of a deep sea fan complex. The Goldenville Formation represents a "proximal" member of a deep sea fan complex Quartz grains in the Goldenville Formation, (Dwyer, 1979) have a larger size than the quartz grains in the Halifax Formation at Ovens Park; paleocurrents of the Goldenville Formation in the area (Campbell, 1966) have a trend that is approximately the same as the trend found at Ovens Park. This "proximal" and "distal" concept is similar to the "proximal" and "distal" concept proposed by Harris and Schenk (1968, 1975). Schenk and Harris suggested that the Goldenville Formation was proximal relative to the Halifax Formation (which was considered a distal deposit).

11. Paleocurrent indicators used to assist in distinguishing the channel facies assemblage from the overbank-interdistributary channel facies suggest the source of sediment was from the south. This conclusion is similar to that of Schenk (1970), and Harris and Schenk (1975) who suggested a south-easterly source area for the sediments.

12. Subfacies D_2 and E_2 are similar to the strata documented by Harris and Schenk (1975) at Black Rock Beach. Harris and Schenk (1975) suggest that the units that they documented may be overbank turbidites (?). A similar conclusion was derived from the data in this thesis, namely, that subfacies D_2 and E_2 represent interchannel turbidite deposits (overbank turbidites).

Bibliography

Allen, J.R.L., 1970, Physical Processes of Sedimentation, Elsevier Publishing Company, Amsterdam, 248 pp.

Ami, H.M., 1900; Synopis of the Geology of Canada; Proc. and Trans. Roy. Soc. Can., New Series, V. 6, p. 1870226.

Bouma, A.H., 1962; Sedimentology of some Flysch Deposits. A Graphic Approach to Facies Interpretation; Elsevier Publ. Co., Amsterdam, 168 pp.

Campbell, F.H.A., 1966; Paleocurrents and Sedimentation of part of the Meguma Group, Lower Paleozoic of Nova Scotia, Canada; Unpubl. M. Sc. Thesis, Dalhousie University, 91 pp.

Campbell, F.H.A., Schenk, P.E., 1967; Paleocurrent and Basin Analysis of the Meguma Group, Nova Scotia; Maritime Sediments, V. 3, p. 27-30.

Cant, D. J., Walker, R.G., 1976;Development of a braided fluvial facies model for the Devonian Battery Point Sandstone, Quebec, Can., J. of Earth Sci., Vol. 13, p. 102-119.

Crosby, D. G., 1962; Wolfville Map Area, Nova Scotia; Geol. Sur. Can. Mem. 325.

Douglas, G. C., Milner, R.L., and MacLean, J., 1938; The Deposition of the Halifax Series; Nova Scotia Department of Public Works and Mines, Annual Report for 1937, pt. 2, p. 34-35.

Dunham, R.J., 1962; Classification of Carbonate Rocks According to Depositional Texture. In Ham , W.E. (ed.); Classification of Carbonate Rocks. Am. Ass. Petrol. Geol. Mem. 1, p. 108-121.

Dwyer, J.D., 1979; Depositional Analysis of a Section of the Lower Meguma (Lower Paleozoic, Ship Harbour, Nova Scotia Unpubl. B.Sc (Honours) Thesis, Dalhousie University, 118 pp.

Dzulynski, S., Walton, E.K., 1965; Sedimentary Features of Flysch and Greywackes; Elsevier Publishing Company, Amsterdam, 274 pp.

Fairbault, E. R., 1914; Greenfield and Liverpool Town map-areas, Nova Scotia Geol. Sur. Can. Summ. Report 1912, p. 334-340.

Fisher, A.R. and Yates, F., 1963; Statistical Tables for Biological Agricultural and Medical Research, Hafner Publishing Company Inc., N.Y., p. 47.

Fyson, W.K., 1966; Structures in the Lower Paleozoic Meguma Group, Nova Scotia, Geol. Soc. of America Bull., V. 77, p. 931-944.

Harbaugh, J. W., Bonham-Carter, G., 1970; Computer Simulation in Geology, John Wiley and Sons, Inc., New York, 575 pp.

Harms, J.C., Fahnestock, R.K., 1965; Stratification, Bed Forms and Flow Phenomena (With and Example from the Rio Grande) In Primary Sedimentary Structures and their Hydrodynamic Interpretation Soc. Ec. Paleon. and Min. Sp. Publ. No. 12, p. 84-115.

Harms, J.C., Southard, J.B., Spearing D. B., Walker, R.G., 1975; Depositional Environments as Interpreted from Primary Sedimentary Structures and Stratification Sequences; Soc. Ec. Paleon. and Min. Short Course. No. 2; Dallas, 161 pp.

Harris, I.M., 1971; Geology of the Goldenville Formation, Taylor Head, Nova Scotia; Unpubl. Ph.D. thesis, Univ. Edinburgh, 226 pp.

Harris, I.M. and Schenk, P.E.,1968; A Study of Sedimentary Structures in the Goldenville Formation, eastern Nova Scotia, Maritime Sediments, V. 4, p. 1-3.

Harris, I.M. and Schenk, P.E., 1975; The Meguma Group, In Harris I.M. (ed.) Ancient Sediments of Nova Scotia, Eastern Soc. Ec. Paleon. and Min. Guidebook 1975 Fieldtrip, p. 17-38.

Hesse, R. and Chough, S.K.,1980; The Northwest Atlantic Mid-Ocean Channel of the Labrador Sea: II. Deposition of Parallel Laminated Levee-muds from the Viscous Sublayer of Low Density Turbidity Currents. Sedimentology, V. 27, No. 6, p. 697-711.

Knapp, R. T. and Bell, H.S., 1941; Density Currents Am. Geophy., Union, Trans., V. 22, p. 257-261.

Kuenen , PH. H., 1951; Mechanics of Varve Formation and the Action of Turbidity Currents, Geol. Føren. Stockh. Førh. 73, 69-84.

Kuenen , PH. H., 1956; The Difference Between Sliding and Turbidity Flow, Deep-Sea Res., V. 3, p. 134-139.

Lowe, D.R., 1975; Water Escape Structures in Coarse Grained Sediments, Sedimentology, 22, p. 157-204.

Malcom, W., 1929; Gold Fields of Nova Scotia; Geol. Surv. Can. Mem. 156.

Miall, A.D., 1973; Markov chain analysis applied to an ancient alluvial plain succession; Sedimentology. Vol. 20, 347-365.

Keppie, J.D. and Muecke, G.K., 1979; Metamorphic Map of Nova Scotia, Nova Scotia Dept. of Mines and Energy.

Middleton, G.V. and Hampton, M.A., 1976; Subaqueous Sediment Transport and Deposition by Sediment Gravity Flows, In Stowley, D. J. and Swift, D.J.P. (ed.): Marine Sediment Transport and Environmental Management, John Wiley, New York, p. 197-218.

Nelson, C.H., 1975; Turbidite Fans and Other Base-of-Slope Deposits. In Dickenson, Wm. R. (ed.) Current Concepts of Depositional Systems with Applications for Petroleum Geology; Short Course - San Joaquin Geological Society p. (6-1): (6-5).

Normark, W.R., Piper, D.J.W., Hess, G.R. 1979; Distributary Channels, Sand Lobes and Mesotopography of Navy Submarine Fan, California Borderland, with Applications to Ancient Fan Sediments, Sedimentology, V. 26, p. 749-774.

Mutti, E., 1977; Distinctive Thin-bedded Turbidite Facies and Related Depositional Environments in the Eocene Hecho Group (South-Central Pyrenees, Spain), Sedimentology, V. 24, pp. 107-131.

Phinney, W.C., 1961; Possible Turbidity Current Deposition in Nova Scotia (Abst.) Bull. Geol. Soc. America V. 72, p. 1453-1454.

Piper, D.J.W., 1972; Turbidite Origin of Some Laminated Mudstones, Geol. Mag., 109; p. 115-126.

Piper, D.J.W., 1973; The Sedimentology of Silt Turbidites from The Gulf of Alaska; Initial Reports of the Deep Sea Drilling Project, Leg. 18, Volume XVIII, Washington, D.C. (U.S. Government Printing Office), p. 847-868.

Piper, D.J.W., and Brisco, C.D., 1975; Deep Water Continental Margin Sedimentation Initial Reports of the Deep Sea Drilling Project Leg 28, Volume XXVIII, Washington, D.C. (U.S. Government Printing Office) p. 727-755.

Piper, D.J.W., 1978; Turbidite Muds and Silts on Deep Sea Fans and Abyssal Plains In Sedimentation in Submarine Canyons, Fans and Trenches (ed. D.J. Stanley and G. Kelling), Dowden, Hutchinson and Ross, Stroudsburg, Pa., p. 163-176.

Reading, H.G., 1978; Facies In Sedimentary Environments and Facies (ed. by H.G. Reading) Blackwell Scientific Publications, London, pp. 4-12.

Rupke, N.S. 1978; Deep Sea Clastics In Reading H.G. (ed.); Sedimentary Environments and Facies, Blackwell Scientific Publications, London, p. 372-415.

Potter, P.E. and Pettijohn, F.J., 1963; Paleocurrents and Basin Analysis; Springer, Berlin, 296 pp.

Schenk, P.E., 1970; Regional Variations of the Flysch-like Meguma Group (Lower Paleozoic of Nova Scotia), Compared to Recent Sedimentation off the Scotian Shelf; In Lajoie, J. (ed.); Flysch Sedimentology in North America Geol. Assoc. Can. Spec. Paper, No. 7, p. 127-153.

Stevenson, I.M., 1959; Shubenacadie and Kennetcook map-areas, Colchester, Hants and Halifax Counties, Nova Scotia, Geol. Soc. Can., Memoir, 302.

Stow, D.A.V. and Lovell, J.P.B. 1979; Contourites, Their Recognition in Modern and Ancient Sediments, Earth-Sci., Rev., V. 14, pp. 251-291.

Stow, D.A.V. and Shanmugam, G., 1980; Sequence of Structures in Fine-grained Turbidites: Comparison of Recent Deep-Sea and Ancient Flysch Sediments; Sedimentary Geology, V. 25, p. 23-42.

Taylor, F.C., 1967; Reconnaissance Geology of the Shelburne map-area, Queen's, Shelburne and Yarmouth Counties, Nova Scotia, Geol. Surv. Can., Mem. 349.

Terry, R.D. and Chilingar, G.V., 1955; Comparison Chart for Estimating Percentage Composition; Jour. Sed. Petrog. V. 25, no. 3, p. 229-234.

Walker, R.G. 1979; Turbidites and Associated Coarse Clastic Deposits, In Walker R.G. (ed.) Facies Models; Geo. Science Canada, Reprint Series 1, Toronto, p. 91-104.

Woodman, J.E., 1904; Nomenclature of the Gold-Bearing Metamorphic Series of Nova Scotia; Am. Geol., V. 33, p. 363-370.

Addentum:

Hobbs, B.D., Means, W.D. and Williams,P.F., 1976;An Outline of Structural Geology, John Wiley and Sons,Inc.,New York.

Gould,H.R.,1951, Some Quantitative aspects of Lake Mead turbidity currents, p. 34-52 IN Hough,J.L.(ed.); Turbidity currents and the transportation of coarse sediments to deep water,Tulsa, Okla., Soc. Econ. Paleon. and Min. Spec.Pub. No.2, 107p.

Appendix 1

(Section 1,Thunder Cave)

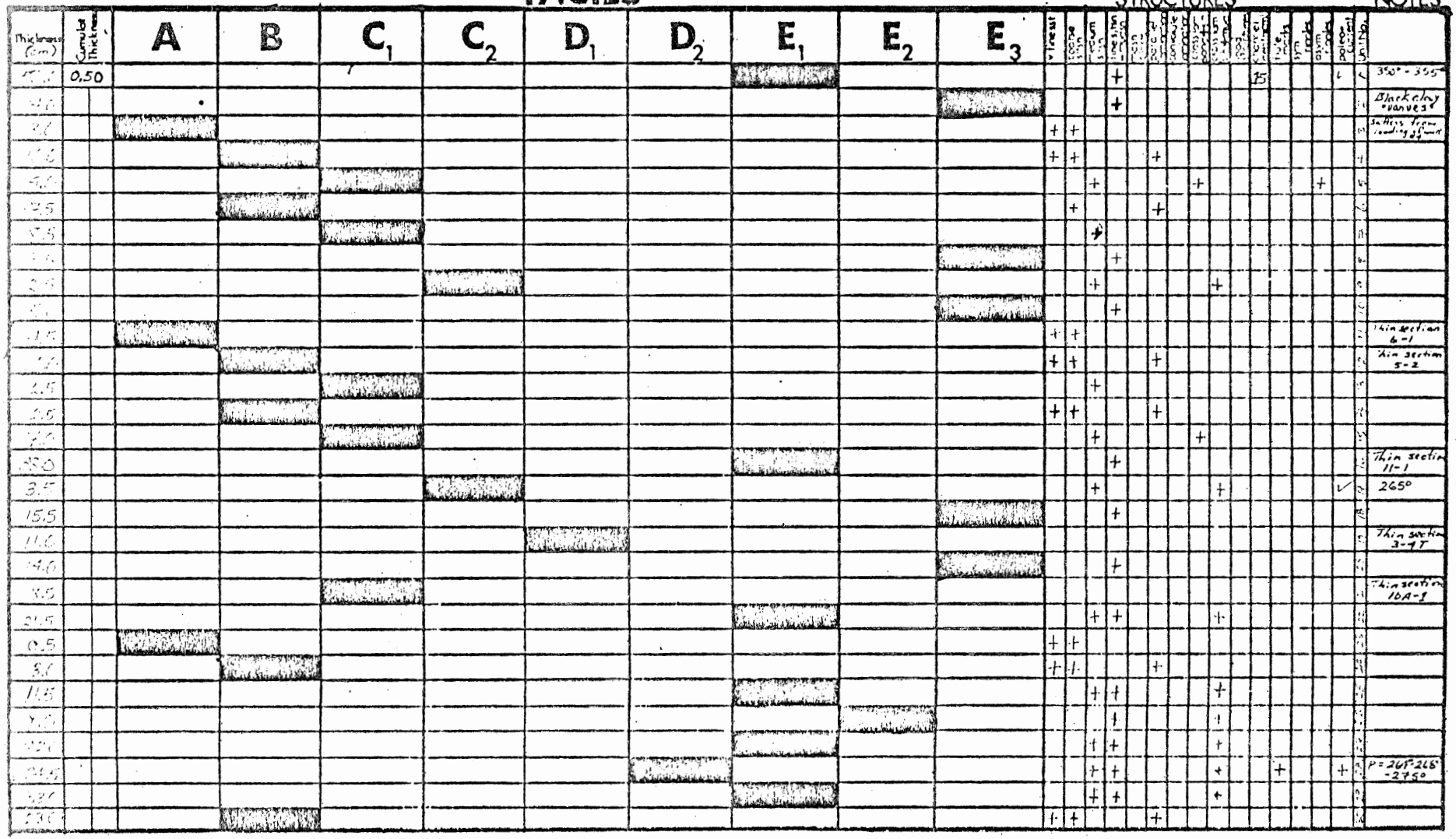
FACIES
STRUCTURES
NOTES
Thickness (cm)
Cumulative Thickness
A
B
C1
C2
D1
D2
E1
E2
E3
0,50
Blackchay "varves"
Thin section 6-1
Thin section 5-2
Thin section 11-1
265°
Thin section 3-7T
Thin section 10A-1
P = 265°-268°-275°

FACIES

Thickness	Cumulative Thickness	A	B	C_1	C_2	D_1	D_2	E_1	E_2	E_3	STRUCTURES	NOTES
970								■			+ +	
[illegible]		■									4 + +	
2.5			■								+ -1 +	
3.0				■							+ +	
[illegible]								■			+ +	
4.5						■					+ +	
[illegible]								■			+	
[illegible]		■									+ + 1	
[illegible]				■							+ +	
[illegible]								■			+ +	
[illegible]						■					+ +	Thin section 3-5B
[illegible]										■	+	
2.0			■								+ +	
[illegible]		■									+	
1.0				■							+ +	
[illegible]		■									+ +	
1.0			■								+ + +	
[illegible]		■									+ + +	Thin section 7-2B
1.0				■							+ + ✓	855° section 7-1B
[illegible]		■									+ +	
[illegible]			■								+ + +	Thin section 3-1
[illegible]		■									1 1	
[illegible]			■								1 1 +	
[illegible]		■									1 1	
[illegible]			■								1 1 +	
[illegible]		■									1 1	Thin section 7-2B
[illegible]			■								+ + +	
[illegible]				■							+ + ✓	360°-css
[illegible]			■								+ + +	
[illegible]		■									1 1	

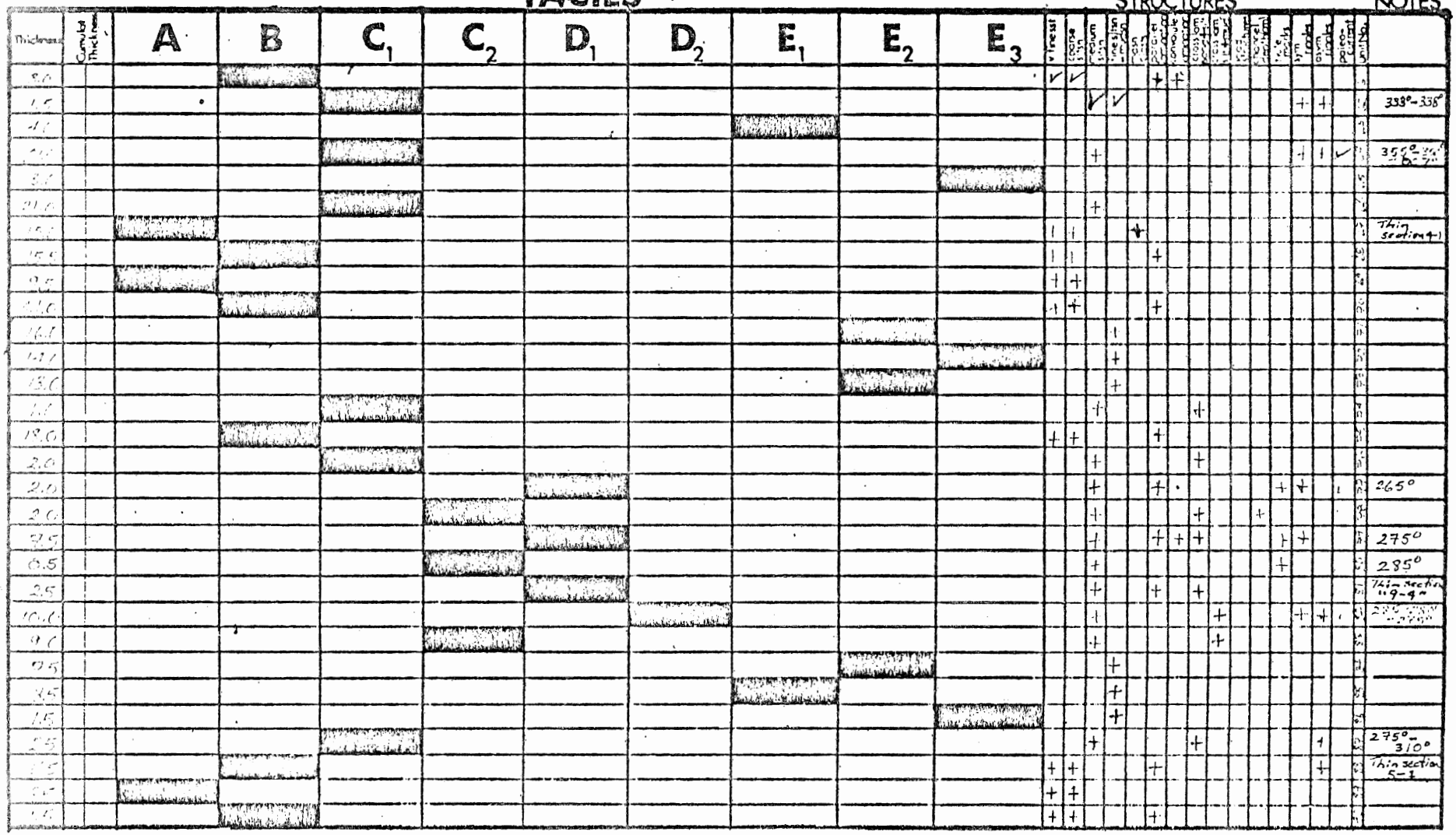
FACIES
STRUCTURES
NOTES
Thickness
Cumulative Thickness
A
B
C1
C2
D1
D2
E1
E2
E3
Thin section 4-1
338°-335°
355°-
265°
275°
285°
Thin section 9-9-
275°-310°
Thin section S-1

FACIES

Thickness	Cumulat. Thickness	A	B	C1	C2	D1	D2	E1	E2	E3	v. fine ss	coarse silt	medium silt	fine silt-clay	rain	parallel laminae	convolute laminae	cross-lam	cross-lam and	[illegible]	channel	flute marks	sym. ripples	asym. ripples	paleo-current	Unit No.	NOTES
3.0							X						+	+					+						✓	[illegible]	235°-255° -270°
2.5									X				+	+												[illegible]	
3.[illegible]						X							+	+			+									[illegible]	
3.5							X						+	+								+			✓	54	272°
4.0									X				+	+												[illegible]	
3.5							X						+									+			✓	[illegible]	292°
0.5									X					+												[illegible]	
[illegible]							X						+	+												[illegible]	
.0						X							+				+									[illegible]	
3.[illegible]									X				+	+												[illegible]	
2.5										X				+												[illegible]	
[illegible]					X								+													[illegible]	Thin section 11-33
5.5							X							+					+							[illegible]	
19.0						X							+													[illegible]	
4.5									X				+													[illegible]	
1.5					X								+						+							[illegible]	
3.5						X								+												[illegible]	
3.5							X						+	+								+			✓	[illegible]	265°
3.5						X							+			+										[illegible]	
2.5							X						+	+												[illegible]	Thin section "Flute Mark"
2.5						X							+													[illegible]	
2.[illegible]					X								+													[illegible]	
1.[illegible]						X							+	+												[illegible]	
2.0										X				+												[illegible]	
1.0						X							+													[illegible]	
3.0							X							+								+			✓	[illegible]	295°
1.0					X								+													[illegible]	
3.5							X							+												[illegible]	
7.5					X								+													[illegible]	
[illegible]							X							+								+			✓	[illegible]	215°

		FACIES									STRUCTURES																NOTES
Thickness	Cumulat. Thickness	A	B	C_1	C_2	D_1	D_2	E_1	E_2	E_3	v fissil	coarse lam	[illegible]	[illegible]	[illegible]	[illegible]	[illegible]	cross [illegible]	[illegible]	[illegible]	channel [illegible]	flute [illegible]	[illegible]	[illegible]	paleo current	[illegible]	
11.0					■								+						+								Thin section "H"
12.5							■						+	+					+			+	+				Thin section H-2
18.5					■								+						+	+							
25			■								+	+															
[illegible]									■					+													[illegible]
[illegible]								■					+	+													
[illegible]							■						+									+					2.75° [illegible]
[illegible]						■							+														
[illegible]								■						+													
[illegible]			■								+	+															
[illegible]				■									+						+					+			275°-215° -325°
[illegible]			■								+	+															
[illegible]				■									+						+					+			275°-325°
8.5			■								+	+															
3.0							■						+	+													
9.5			■								+	+															
9.5								■					+	+													
23.5									■					+													lenticular "beds"
[illegible]							■						+	+													
[illegible]								■						+													
[illegible]						■							+	+			+					+					
[illegible]								■						+													
[illegible]						■							+	+								+					
[illegible]								■						+													
[illegible]						■							+	+								+					
[illegible]													+	+													
[illegible]						■							+				+					+					
[illegible]									■					+													"bulbous" layers
[illegible]							■						+	+								+					
5.0								■						+													

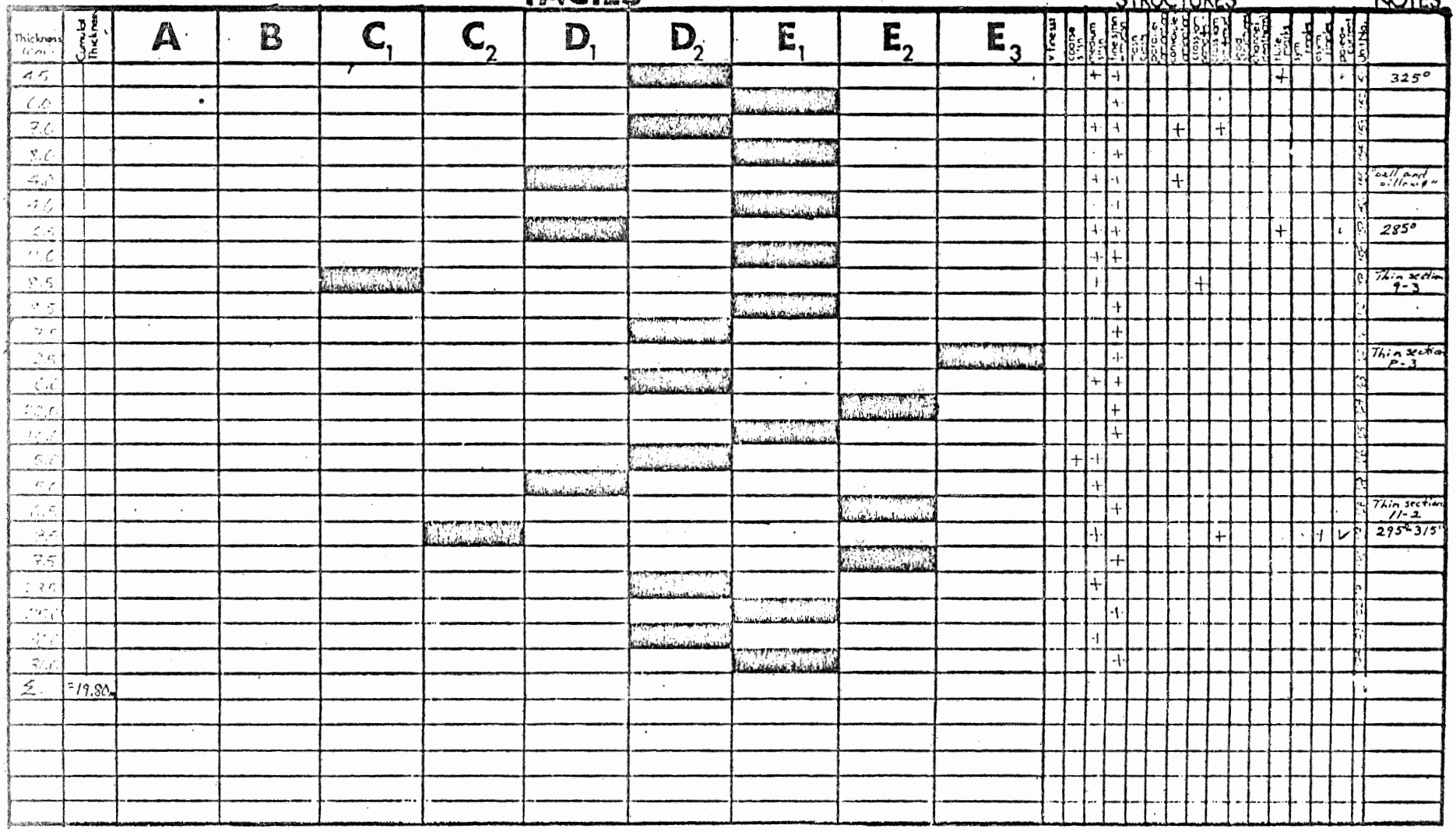
FACIES
STRUCTURES
NOTES
Thickness (cm)
Bed Thickness
A
B
C1
C2
D1
D2
E1
E2
E3
Σ = 19.80
325°
285°
Thin section 9-3
Thin section P-3
Thin section 11-2
295° & 315°

Appendix 2
(Section 2, Ovens Park Beach)

FACIES / STRUCTURES / NOTES

Thickness (cm/inches)	Cumulat. Thickness	A	B	C1	C2	D1	D2	E1	E2	E3	v fine sst	coarse sltsn	medium sltsn	fine sltsn + mdstn	mdstn clasts	parallel lamination	convolute lamination	cross lam. sand+silt	cross lam. silt+mud	load structures	channel deposits	flute marks	sym ripples	asym ripples	paleo-current	Unit No.	NOTES
24.1	24.1m								■				+	+				+						+	✓	1	350–310° –320°
23.0					■								+													2	
56.0							■						+	+				+								3	
4.0					■								+													4	
22.0									■					+					+							5	
10.0					■								+						+							6	
51.0						■							+	+			+		+							7	
38.0				■									+													8	
97.0								■					+													9	
7.0									■					+												10	
25.0								■					+													11	
8.0					■								+						+					+	✓	12	350°
10.0							■						+													13	
8.0									■					+												14	
7.0							■						+													15	
5.0									■					+												16	
17.0							■						+	+												17	
9.0										■				+												18	
2.5					■														+							19	
5.5									■				+	+												20	
18.0										■				+												21	
3.0					■														+					+	✓	22	275°–340° –350°
48.0									■				+	+												23	
11.0										■				+												24	
26.0					■														+							25	
20.0										■				+												26	
9.0					■														+					+	✓	27	275°–295° 340°
32.0									■					+												28	
12.0						■												+								29	
28.0									■					+												30	

FACIES

Thickness (cm)	Cumulat Thickness	A	B	C1	C2	D1	D2	E1	E2	E3	v fine sst	coarse sltsn	medium sltsn	fines sltsn - mdstn	massive clasts	parallel lamination	convolute lamination	cross lam. sand-silt	cross lam. silt-mud	load structures	channel depth (cm)	flute marks	sym ripples	asym ripples	paleo-current	Unit No.	NOTES
45.0								■						+												31	
23.0									■					+												32	lenticular "Beds"
3.0					■								+													33	
30.0									■				+	+												34	
11.0							■						+					+								35	
10.0									■					+												36	/
2.5					■								+					+								37	
19.5									■					+												38	
3.5					■								+					+								39	
19.0									■					+												40	
6.0					■								+					+								41	
5.0										■				+												42	
2.5					■								+					+								43	
28.0									■					+												44	bulbous "beds"
3.5							■						+	+				+								45	
11.5									■					+												46	
3.0					■								+													47	
15.0									■					+												48	
42.0							■						+					+								49	
40.0									■					+												50	bulbous "beds"
10.0							■						+					+								51	
38.0									■					+												52	
13.5							■						+					+								53	
32.0								■						+												54	
7.0							■						+					+								55	
10.0								■						+												56	
19.0							■						+													57	
13.5									■				+	+												58	
5.0							■						+	+												59	
30.0									■					+												60	

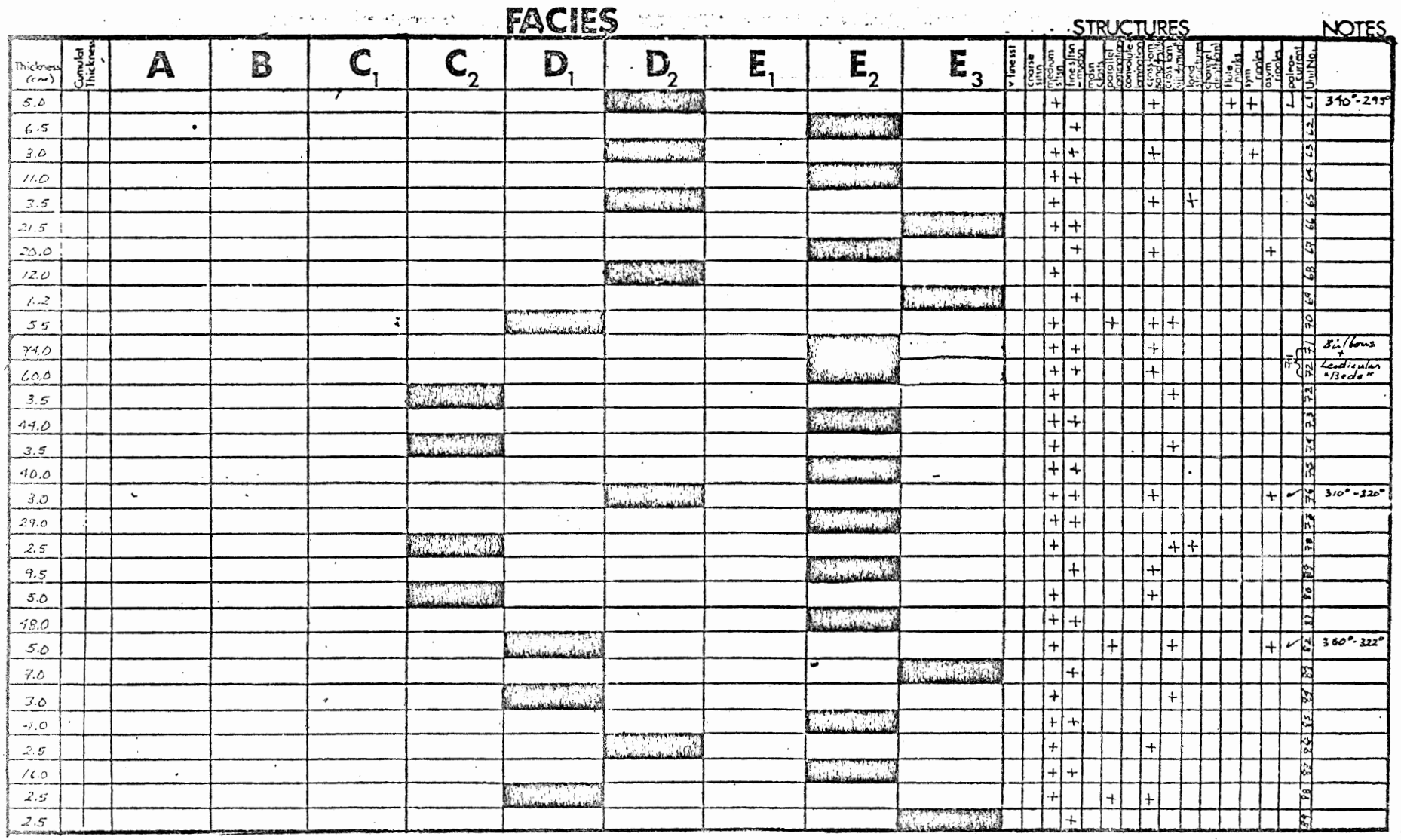
FACIES
STRUCTURES
NOTES
Thickness (cm)
Cumulat Thickness
A
B
C1
C2
D1
D2
E1
E2
E3
v fine ss
coarse silt
medium silt
fine silt - mudst
mdstn laminae
parallel laminae
convolute lamination
cross lam
ripple drift cross lam
flute marks
sym ripples
asym ripples
load structures
pelecypod shells
Unit No.
5.0
6.5
3.0
11.0
3.5
21.5
20.0
12.0
1.2
5.5
74.0
60.0
3.5
44.0
3.5
40.0
3.0
29.0
2.5
9.5
5.0
48.0
5.0
7.0
3.0
41.0
2.5
16.0
2.5
2.5
340°-295°
Bivalves + Lenticular "Beds"
310°-320°
360°-322°

FACIES

Thickness (cm)	Cumulat Thickness		A	B	C_1	C_2	D_1	D_2	E_1	E_2	E_3	v finesst	coarse sltsn	medium sltsn	finesltsn -mdsn	mdsn clasts	parallel lamination	convolute lamination	cross lam sand+silt	cross lam silt+mud	load structures	channel	flute marks	sym ripples	asym ripples	paleo-current	Unit No.	NOTES
2.5							■							+					+								90	
6.0									■					+	+												91	
1.5											■				+												92	
1.5							■							+			+				+						93	
1.0											■				+												94	
1.5							■							+	+				+	+							95	
308.0										■					+												96	
6.0						■								+					+	+							97	
[illegible]											■				+												98	
12.0								■						+	+												99	
7.0										■					+												100	
2.5						■								+	+				+	+							101	
21.5										■					+												102	lenticular + bulbous bed
2.5						■								+					+								103	
38.0										■					+												104	
3.5					■									+					+						+	✓	106	295°–305°
12.0										■					+												105	
5.5								■						+													107	
4.0										■					+												108	
1.0							■							+	–					+							109	
2.3										■					+												110	lenticular + bulbous beds
2.5								■						+	+												111	
15.0										■				+	+												112	
2.5								■						+													113	
3.5											■				+												114	
2.5								■						+													115	
[illegible]										■				+	+												116	
2.0						■								+						+					+	✓	117	295–305° – 335°–320°
5.0										■				+	+												118	
5.0						■								+						+							119	

FACIES

Thickness (cm)	Cumulat Thickness	A	B	C_1	C_2	D_1	D_2	E_1	E_2	E_3
11.0										
2.0										
99.0										
3.0										
21.0										
4.0										
20.0										
9.0										
16.0										
3.0										
2.0										
2.0										
4.5										
2.5										
10.0										
11.5										
31.0										
16.0										
3.0										
22.0										
9.0										
9.0										
5.5										
2.0										
16.0										
20.0										
3.0										
8.0										
2.0										
12.0										

STRUCTURES

v finest	coarse silt/sn	medium s/sn	fine/silt/sn - mudst	massive	obscure	parallel	undulose	convolute	cross-lam	cross-bed	silt + mud	load structures	channel deathmt	flute marks	syn ripples	asym ripples	paleo-current	Unit No.
		+	+															120
		+																121
			+															122
		+								+								123
			+															124
		+																125
			+															126
		+								+								127
			+															128
		+																129
			+															130
		+																131
			+															132
		+								+								133
			+															134
		+																135
		+	+															136
		+																137
			+															138
		+								+								139
			+															140
		+																141
		+	+															142
		+									+							143
		+																144
			+															145
		+																146
			+															147
		+																148
		+	+															149

NOTES

stained ripples??

FACIES

Thickness (cm)	Cumulat Thickness	A	B	C_1	C_2	D_1	D_2	E_1	E_2	E_3	v fine sst	coarse siltst	medium siltst	fine siltst + mudst	mudst clasts	parallel lamination	convolute lamination	cross-lam sand+silt	cross-lam silt+mudst	load structures	channel (distal)	flute marks	sym ripples	asym ripples	paleo-current	Unit No.	NOTES
12.0							■						+	+					+							150	
13.0									■				+	+												151	
2.0					■								+						+							152	
53.0									■					+												153	
23.0							■						+							+						154	
2.0									■					+												155	
5.0					■								+						+							156	
2.0									■					+												157	
19.0							■						+						+					+	✓	158	342°-300°
10.0					■								+													159	
2.0									■					+												160	
17.0							■						+	+												161	
5.0					■								+					+								162	
1.5									■					+												163	
8.0					■								+					+								164	
2.0									■					+												165	
7.0					■								+													166	
16.0							■						+						+					+	✓	167	295°-275° 265°-340°
1.5									■					+												168	
3.0					■								+					+								169	
1.5									■					+												170	
3.0					■								+													171	
19.0							■						+						+					+	✓	172	345-300 -275°
2.0									■				+												—	173	
2.0							■						+													174	
Σ =	29.93m																										

Appendix 3
(Bar Graphs Showing the Grain Size
Distribution in Facies A,B,C,D
and E)

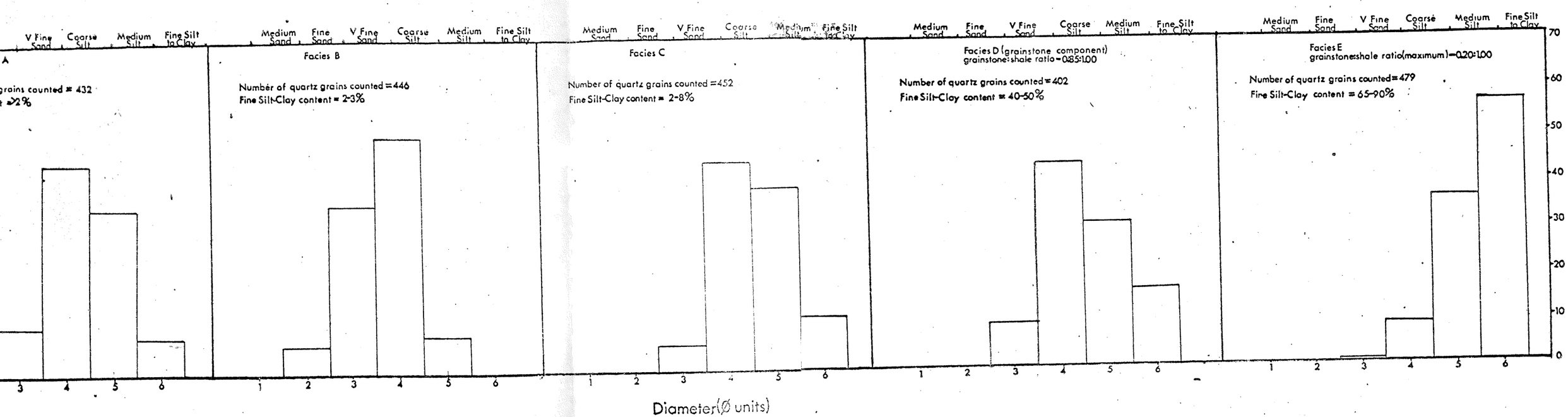

Approximate Size Distribution of Quartz
Grains in the Facies Units at Thunder Cave

he clay content was estimated by visual analysis by using the "Comparison Chart for Estimating ercentage Composition"(Richard, T. and Chlinger, G.V., 1955) as a standard reference.

ne hundred and fifty quartz grains were counted per thin section in a suite of three thin sections hat were chosen to be representative samples of the grain size fabric of each facies. All the amples used to produce the thin sections were taken from the Thunder Cave section (Refer to Appendix for sample locations).

APPENDIX 3

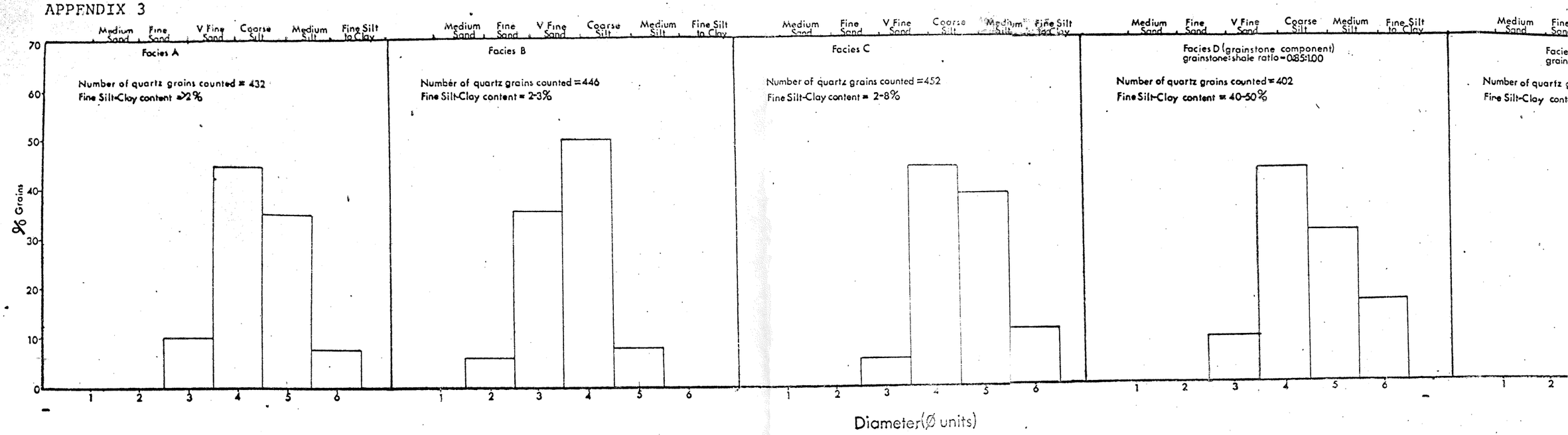

Approximate Size Distribution of Quartz
Grains in the Facies Units at Thunder Cave

Note - 1: The clay content was estimated by visual analysis by using the "Comparison Chart for Estimating Percentage Composition"(Richard, T. and Chlinger, G.V., 1955) as a standard reference.

2: One hundred and fifty quartz grains were counted per thin section in a suite of three thin sections that were chosen to be representative samples of the grain size fabric of each facies. All the samples used to produce the thin sections were taken from the Thunder Cave section (Refer to Appendix 1 for sample locations).

Appendix 3A

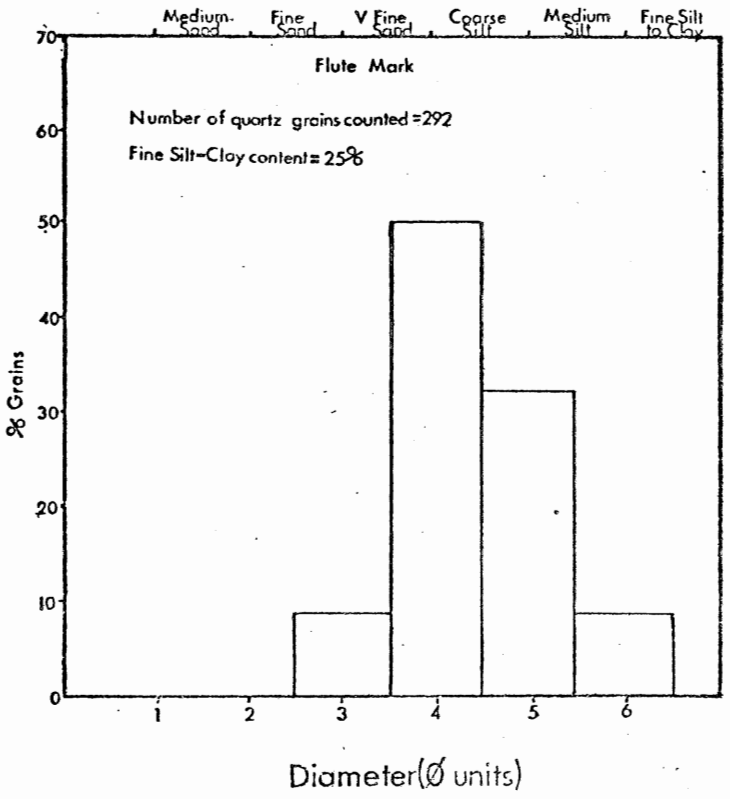

Approximate Size Distribution of Quartz Grains in a Flute Mark from a Facies D Unit.

Note: The clay content was estimated by visual analysis by using the "Comparison Chart for Estimating Percentage Composition" (Richard, T. and Chlinger, G.V., 1955) as a standard reference.

Appendix 4

(A Description of First Order Markov Chain Analysis)

Markov Chain Analysis - First Order

Natural processes that are random in their occurrence also exhibit an effect in which previous events influence, but do not rigidly control, subsequent events, these are referred to as Markov processes. A Markov process is a process in which the probability of the process being in a given state at a particular time may be deduced from knowledge of the immediately preceding state. A form of a Markov process is a Markov chain, which may be regarded as a sequence chain of discrete states in time in which the probability of the transition from one state to a given state in the next step in the chain depends upon the previous state.

A Markov chain may be regarded as a series of transitions between different states such that the probabilities associated with each transition depend only on the immediately preceding state and not on how the process arrived in that state. The general form of a Markov chain is such that it contains a finite number of states and the probabilities associated with the transitions between states are stationary. The transitions have a very short memory, extending for only a single step at a time and ceasing beyond that step. If the probabilities associated with each transition are extended so that events associated with each transition depend on events earlier than the immediately preceding event the Markov chain is a higher order chain.

An event in a Markov association can be expressed as a probability simply by dividing that event by the total number of events to which that event is associated. Estimates of probability values can be substituted for the events listing the transition frequencies. These probability values are termed Markov transition probabilities. These probabilities can be ordered into a transition matrix, in which the number of rows equals the number of columns corresponding to the number of states. The probability value of each row sums to one (1), which, in effect, says that there is absolute certainty of a transition from each state to some state in the next event in the chain of finite events.

Markov processes can be classified into two groups 1) Discrete time, and 2) continuous time. Both of these groups can be subdivided to discrete state and continuous state subgroups.

Markov probability matrices provide a succinct description of the behavior of a Markov chain. Each element in the matrix represents the probability from a particular state to the next state.

The aspect of memory in a Markov chain involves conditional probability; this implies that the probability of a particular event is conditional on some other event. Consider probability independent of other events; Pr[x] additional information is received that modifies the probability. The probability of y upon receipt of x is: Pr[y/x] which is the probability of y, given x. Markov chains are one way

of dealing with sequences of events whose probabilities are conditional on some other event.

Transitions in any series of observations that involve either discrete-state or discrete-time phenomena can be described by a matrix of transition probabilities provided that there is a finite number of states in the system.

A statistical test for the Markov property forms an important component of the tools of the experimenter. The test distinguishes between the two alternative hypothesis that either the successive events are independent of each other (the null hypothesis) or events are not independent. If not independent, they can form a first order Markov chain. Using the equation presented in Section IV and the degrees of freedom presented in Section IV, and if we make the level of significance $\alpha = 0.05$, a table of X^2 values can be consulted. If the value of the test equation is much greater than the X^2 value, the null hypothesis can be rejected (i.e., independent event processes) and we can accept that the transitions have the Markov property.

Estimated Time Spent on Thesis:

Mapping and Field Work

12 days - fall '80 - winter '81 - mapping and logging sections

3 days - notes, photos

Laboratory

1 week - polishing slabs of block samples

2 days - describing sedimentary structures

Reading

Summer 1980, fall 1980, winter 1980-81 - time permitting -

for background research

Writing

Winter 1980 - time permitting

Winter 1981 - 8 weeks (time permitting).